Dynamic Rate Analysis for

Low Frequency Operation of Chemical Reactors

Austin Morales, Praveen Bollini, and Michael P. Harold⁺

William A. Brookshire Department of Chemical and Biomolecular Engineering

Houston, TX 77204-4004

⁺ Corresponding Author; mharold@uh.edu

Abstract

Periodic operation of chemical reactors can enhance reactant conversion and product selectivity. It is desirable to identify reaction kinetics and networks that may benefit from non-steady state operation and to quantify the extent of that enhancement without extensive computations. In this study, we describe a simple method to establish approximate functional dependencies of isothermal point reaction enhancement on dynamic and kinetic parameters during low frequency operation. Low frequency operation permits the use of steady state as opposed to transient conservation equations to identify limits of fractional rate enhancement. By approximating local dynamic rates as square waves modulating between two steady states, an analytical function can be derived from global rate expressions. The function relates fractional rate enhancement to concentration wave amplitudes, phase shifts, cyclic averages, duty cycles and reaction orders for one or more dynamically-fed reactants. We show that the method may be applied to predict integral conversion enhancement for ideal reactors. During integral operation, nonstoichiometric concentration waves may change phase through disproportionate consumption of reactants at wave maxima and minima hence inverting waves out-of-phase (180°) from their initial waveform. This may cause local rate enhancement to transition to rate diminishment. Three experimental examples involving catalytic oxidations are described that illustrate selected theoretical aspects of the study.

Keywords: Rate; Modulation; Periodic; Quasi Steady State; Forced Dynamic; Reactor

1. Introduction

Non steady state operation of chemical reactors through periodic operation can improve reactant conversion and desired product selectivity over levels achieved using conventional steady state (SS) operation [1][2][3][4][5][6][7]. However, the mathematical complexity associated with transient reactor operation thwarts the determination of reaction network type, kinetics and operating conditions leading to performance enhancement [1][2][3]. This has inspired development of methods that identify regions of dynamic enhancement, and quantify the extent of enhancement obtained under a given set of conditions [3][8][9].

Cyclic modulation of the reactant concentration will result in a higher cyclic average rate compared to steady state operation if the reaction rate has a convex dependence on the reactant concentration [3][10]. The opposite trend will occur for a concave rate dependence [3][10]. This effect is graphically demonstrated by drawing a chord between the concentration maxima and minima on a rate versus concentration diagram [3][10]. If the chord falls above the rate versus concentration curve, the cyclic average dynamic rate will exceed the steady state whereas if the chord falls below the curve the dynamic rate will be less than the steady state [3][10]. This feature is restricted to the effect on the instantaneous rate from a single dynamically operated reactant with a period much larger than the response time of the system [3][10]. Specifically, Bailey states that this occurs when the ratio of the reactor time scale (residence time) to oscillation time scale (cycle period) is greater than 100 [11][12]. This restriction implies that the system approaches steady state at each maximum and minimum of the concentration wave [3]. Silveston and others referred to such modes of operation as being in the quasi-steady state (QSS) regime [2][3][10].

Bailey and coworkers explored this concept by demonstrating higher intermediate product yields during the modulation of multiple reactants compared to single reactant modulation and

steady state operation for a consecutive reaction network [13]. Others have reported enhanced reactor performance during the periodic operation of multiple reactants [8][9][14].

Optimization techniques such as the Pi-Criterion and related variational methods have been shown to predict process enhancement in periodically operated continuous stirred tank and batch reactors [15][16][17][18][19][20]. Others including the groups of Morgenstern, Petkovska and Rippin have studied modular concentration, temperature and flow profiles to analyze the effects of periodic parameters on process performance [21][22][23][24][25][26]. Further studies accounting for surface dynamics such as adsorption, desorption and reactions over catalyst surfaces also demonstrate improvement during cyclic operation [26][27].

In this study, we develop a simple method to identify regions of rate enhancement using global kinetics. The method applies a simple expression for the local (differential) fractional rate enhancement as a function of dynamic parameters for one or more dynamically operated reactants during isothermal QSS operation. The method is extended to integral operation in ideal reactor types (PFR and CSTR) for single and sequential reaction schemes, respectively. We show how local rate enhancement translates to integral properties such as conversion and yield. We demonstrate that the theoretically predicted rate enhancement is in agreement with that measured during the periodic operation of ethane and oxygen during total oxidation over a nickel spinel catalyst. Finally, we illustrate a case of oxygen concentration wave inversion during the oxidative dehydrogenation (ODH) of ethane to ethylene over a MoO_x Al₂O₃ catalyst.

2. Results and Discussion

2.1 Quasi-Steady State Dynamic Local Rate Analysis

We consider the case of an isothermal chemical reaction having a power law rate dependence on the concentration of N reacting species:

$$r = k_{eff} \prod_{i=1}^{N} C_i^{n_i} \tag{1}$$

where n_i is the reaction order with respect to species i. Under dynamic conditions, the reactant feed concentrations $C_i(\xi = 0)$, where ξ is the dimensionless distance in a PFR (or time in a batch reactor) are considered square pulses with amplitude above $(C_{i,+}^f)$ and below $(C_{i,-}^f)$ the average concentration $(C_{i,Avg}^f)$ with a period τ and duty cycle s^f , as described by:

$$C_{i}^{f}(t) = \begin{cases} C_{Avg,i}^{f}(1 + \alpha_{+,i}^{f}); \ l \ \tau \leq t < \tau \ (s^{f} + l) \\ C_{Avg,i}^{f}(1 - \alpha_{-,i}^{f}); \ \tau \ (s^{f} + l) \leq t < \tau \ (l + 1) \end{cases} \qquad l = 0, 1, 2 \dots$$
 (2)

A visual interpretation of the above parameters are provided in the Supplementary Information (SI). The dimensionless amplitude of species i $(\alpha_{+/-,i})$ is defined as the amplitude normalized by the average:

$$\alpha_{+/-,i} = \frac{C_{+/-,i}}{C_{Avg,i}} \tag{3}$$

For example, a minimum dimensionless amplitude of 1 ($\alpha_{-}=1$) indicates on-off ("bang-bang") modulation whereas $\alpha_{-}=\alpha_{+}=0$ indicates no modulation. The duty cycle (0 < s < 1) is the fraction of the period (τ) during which the input concentration resides at its maximum value. Conversely, 1-s is the fraction of the period during which the input is at its minimum.

The cyclic average concentration at any point (ξ) in the reactor is defined by

$$C_{Avg,i}(\xi) = \frac{1}{\tau} \int_{t}^{\tau+t} C_i(\xi, t) dt$$
 (4)

Combining Eqn. (2) with Eqn. (4) gives the constraint relating α_+^f , α_-^f and s^f as

$$\frac{\alpha_+^f}{\alpha_-^f} = \left(\frac{1}{s^f} - 1\right) \tag{5}$$

This fixes the integral average of the feed concentration by adjusting the maxima (α_+^f) and minima (α_+^f) according to the duty cycle (s^f) . For example, if the duty cycle is small $(s^f \to 0)$, the input resides at the minimum concentration for a larger fraction of the period. Therefore, a larger α_+^f/α_-^f is required to maintain an equivalent cyclic average. This relationship between the maxima, minima and duty cycle is further illustrated in the SI Fig. S3.1d.

We define the fractional enhancement (Δ) at any point (ξ) in the reactor as

$$\Delta(\xi) = \frac{1}{\tau} \int_{t}^{\tau+t} \frac{r_{QSS}(\xi, t)}{r_{SS}(\xi)} dt - 1$$
 (6)

When $\Delta > 0$ the reaction rate experiences dynamic enhancement, while if $\Delta < 0$, there is dynamic hindrance. For example, $\Delta = -0.3$ means that the cyclic average dynamic rate is 30% less than the steady state rate. It is important to note that Δ is a local parameter as it compares the rate in a QSS reactor to that in a SS reactor at the same point ξ .

The fractional enhancement for the power law reaction rate under QSS operation is obtained by substituting the concentration profile (Eqn. (2)) and rate expression (Eqn. (1)) into Eqn. (6), giving:

$$\Delta = \left(\prod_{i=1}^{N} \frac{C_{i,Avg}^{n_i}}{C_{i,SS}^{n_i}}\right) \left(\prod_{i=1}^{N} \left(1 + \alpha_{+,i}\right)^{n_i} s + \prod_{i=1}^{N} \left(1 - \alpha_{-,i}\right)^{n_i} (1 - s)\right) - 1 \tag{7}$$

Here we have removed reference to position but stress that Δ is a local performance metric. The SI provides a detailed derivation. In Eqn. (7), the cyclic average concentration $(C_{i,Avg})$ is the integral average of the periodic concentration wave (Eqn. (4)), while the steady state concentration $(C_{i,SS})$ refers to the steady state value chosen for comparison. If we assume that the cyclic average feed concentration is equivalent to the steady state concentration $(C_{Avg,i} = C_{SS,i})$, implying that the concentration wave is oscillating around the steady state value, the expression simplifies to

$$\Delta = \left(\prod_{i=1}^{N} \left(1 + \alpha_{+,i} \right)^{n_i} s + \prod_{i=1}^{N} \left(1 - \alpha_{-,i} \right)^{n_i} (1 - s) \right) - 1$$
 (8)

Eqn. (8) assumes that all species have fixed reaction orders, are modulated in-phase, and have the same period and duty cycle. For species that are modulated out-of-phase with a 50% duty cycle (s = 0.5), the fractional enhancement is given by:

$$\Delta = \left(\prod_{i=1}^{N} \frac{C_{i,Avg}^{n_i}}{C_{i,SS}^{n_i}}\right) \left(\prod_{j=1}^{M} \frac{C_{j,Avg}^{m_j}}{C_{j,SS}^{m_j}}\right) \left(\prod_{i=1}^{M} (1+\alpha_i)^{n_i} \prod_{j=1}^{M} (1-\gamma_j)^{m_j} + \prod_{i=1}^{N} (1-\alpha_i)^{n_i} \prod_{j=1}^{M} (1+\gamma_j)^{m_j}\right) - 1$$
(9)

If the cyclic average and steady state concentrations are the same (i.e., the concentration is oscillating around the steady state), then we have

$$\Delta = \frac{\left(\prod_{i=1}^{N} (1 + \alpha_i)^{n_i} \prod_{j=1}^{M} (1 - \gamma_j)^{m_j} + \prod_{i=1}^{N} (1 - \alpha_i)^{n_i} \prod_{j=1}^{M} (1 + \gamma_j)^{m_j}\right)}{2} - 1 \tag{10}$$

where α_i and γ_j represent the dimensionless amplitudes of N total in-phase and M total out-ofphase species in the feed, respectively.

Power law rate expressions are often inadequate in describing the rates over a wide range of concentrations. For example, power law expressions do not account for a shift in the apparent orders. In such cases use of a Langmuir-Hinshelwood-Hougen-Watson (LHHW) rate expression may be necessary. The QSS analysis can be extended to LHHW rate expressions. Here we consider the following catalytic sequence:

 $A_1 + * \leftrightarrow A *_1$

...
$$A_N + * \leftrightarrow A *_N$$

$$A *_1 + \cdots + A *_N \to C *_1 + \cdots + C *_I$$

$$C *_1 \leftrightarrow C_1 + *$$

$$C *_L \leftrightarrow C_L + *$$

where N and L are the number of reactants and products, respectively Assuming adsorption and desorption steps are quasi-equilibrated, and the surface reaction is rate limiting, it can be shows that the LHHW rate expression takes the following form:

$$r = \frac{k_{eff} \prod_{i=ads}^{N} C_i K_i}{\left(1 + \sum_{j=surface}^{M} K_j C_j\right)^N} \tag{11}$$

where M is the number of surface species (M = L + N). The resulting expression for fractional enhancement assuming equivalent duty cycles and in-phase modulation is given by:

$$\Delta = \frac{\left(\frac{s \prod_{i=ads}^{N} (1 + \alpha_{+,i})}{\left(1 + \sum_{j=surface}^{M} K'_{j} (1 + \alpha_{+,j})\right)^{N}} + \frac{(1 - s) \prod_{i=ads}^{N} (1 - \alpha_{-,i})}{\left(1 + \sum_{j=surface}^{M} K'_{j} (1 - \alpha_{-,j})\right)^{N}}\right)}{\left(1 + \sum_{j=surface}^{M} K'_{j}\right)^{-N}} - 1$$
(12)

where,

$$K_j C_{Avg,j} = K_j' \tag{13}$$

Details of the derivation are provided in SI 1.2. The inhibition terms add a new layer of complexity and dependence on the equilibrium adsorption constant and cyclic average of the concentration waves. The larger the value of K'_j the more impactful the denominator terms are on the QSS rate. In the limit of $K'_j \to 0$, Eqn. (12) resembles Eqn. (8) with $n_i = 1$. Increasing the importance of inhibition terms by increasing K'_j results in apparent reaction orders transitioning from being positive to negative, an effect captured by Eqn. (12), but not Eqn. (8). Implications of rate inhibition on QSS reactor performance are explored in later section.

2.2 QSS Dynamic Rate Analysis: Bimolecular Reactions

Consider the modulation of two reactants with a duty cycle of 50% (s = 0.5) for the power law rate expression

$$r = k_{eff} C_1^{n_1} C_2^{n_2} \tag{16}$$

The expression for fractional enhancement during in-phase (simultaneous) modulation is given by

$$\Delta = \frac{(\alpha + 1)^{n_1}(\beta + 1)^{n_2} + (1 - \alpha)^{n_1}(1 - \beta)^{n_2}}{2} - 1 \tag{17}$$

Figs. 1a - c show the enhancement for in-phase (simultaneous) concentration modulation as a function of the dimensionless amplitudes for species 1 (α) and species 2 (β) for three different reaction order cases (n_1 and n_2) and s=0.5. The first case involves one negative and one fractional apparent order for which the sum of orders is less than 0: (a) $n_1 + n_2 < 0$ and $n_1 < 0 < n_2 < 1$. The second case considers two fractional apparent orders with a sum is greater than unity: (b) $n_1 + n_2 > 1$ and $0 < n_1 & n_2 < 1$. The third case considers a reaction with apparent orders less than zero and greater than one which have a fractional sum: (c) $0 < n_1 + n_2 < 1$, $n_2 < 0 & n_1 > 1$.

For the first case (Fig. 1a) the reaction orders are fractional with one negative ($n_1 = -0.4$) and the other positive ($n_2 = 0.2$). The results demonstrate the expected effect of concavity based on the reaction order sign and magnitude. Modulation of species 1 enhances the rate since the order is negative. Modulation of species 2 hinders the rate since the order is positive but less than 1. As the rate is further hindered by increasing the normalized amplitude of species 2 (β), a higher normalized amplitude of species 1 (α) is required to combat the negative effects from the fractional order of species 2.

For the second case (Fig. 1b) the reaction orders are both fractional and positive ($n_1 = 0.7$, $n_2 = 0.9$) with their sum exceeding unity. If either species 1 or 2 are modulated individually while

the other is held at steady state (i.e., $\beta = 0$ and $\alpha > 0$ or vice versa), the rate is hindered. This is expected as each species individually has a fractional rate order and therefore concave rate dependence. However, there exists a large region of rate enhancement along the diagonal. This shows that the combined order $(n_1 + n_2)$ is the key parameter. Consider the diagonal for which the dimensionless amplitudes of 1 and 2 are identical $(\alpha = \beta)$. Applied to Eqn. (17) gives the result

$$\Delta = \frac{(\alpha + 1)^{n_1 + n_2} + (1 - \alpha)^{n_1 + n_2}}{2} - 1 \tag{18}$$

We see that the system behaves as the case of a single reactant with order $n_1 + n_2$. The sum of n_1 and n_2 being 1.6 (>1) and therefore convex with respect to the lumped concentration, results in a higher cyclic average rate compared to the steady state. This result was recently considered by Gottlieb et al. [14]. Grabmuller and Hoffman [8] also found that such combinations of reaction orders $(n_1 + n_2 > 1)$ yield a convex function leading to increased conversion in a periodically operated PFR. This work provides the criterion of equivalent dimensionless amplitudes and duty cycles to achieve enhancement through simultaneous modulation.

The third case (Fig. 1c) is the converse of case 2; in-phase modulation in this case hinders the rate even though individual modulation is beneficial. Here, the species 1 order exceeds unity $(n_1 = 1.2)$ while the species 2 order is negative $(n_2 = -0.5)$. The sum of the reaction orders being fractional (0.7) means that in-phase modulation is detrimental to the overall rate even though the rates are enhanced when either species is modulated individually.

The fractional rate enhancement for a power law rate expression where N reactants are modulated in-phase with approximately equivalent duty cycles $(s_1 \approx s_2 \approx \cdots \approx s_N)$ and dimensionless amplitudes $(\alpha_1 \approx \alpha_2 \approx \cdots \approx \alpha_N)$ is as follows

$$\Delta = \left(s_N (1 + \alpha_N)^{\sum_{i=1}^N n_i} + (1 - s_N)(1 - \alpha_N)^{\sum_{i=1}^N n_i} \right) - 1$$
 (19)

Additional analyses for out-of-phase modulation are shown in SI 3.2. Here, the QSS dynamic rate enhancement for a 50% duty cycle (s = 0.5) during out-of-phase modulation is given by

$$\Delta = \frac{(\alpha + 1)^{n_1} (1 - \beta)^{n_2} + (1 - \alpha)^{n_1} (\beta + 1)^{n_2}}{2} - 1 \tag{20}$$

The terms cannot be mathematically combined in this case, meaning that enhancing effects are not observed as for the case of simultaneous modulation.

Up to this point, we have demonstrated the requirements for local rate enhancement through modulation of multiple reactant concentrations. For example, in the case of simultaneous modulation of two reactants using equivalent dimensionless amplitudes and duty cycles, when the sum of apparent reaction orders exceeds unity, a pronounced enhancement may be encountered. QSS operation where dimensionless amplitudes and duty cycles are not equivalent merely abides by the concavity of the rate function and its dependency on individual reactant concentrations. Next, we extend our analysis to non-power law, Langmuir Hinshelwood kinetics.

2.3 OSS Dynamic Rate Analysis: Langmuir Hinshelwood Hougen Watson Kinetics

We now consider a reaction described by LHHW kinetics for the case of two inhibiting reactants modulated in or out of phase with equal duty cycles. The fractional enhancement is given by

$$\Delta = \frac{\left(\frac{(1+\alpha)(1\pm\beta)}{\left(1+K_1'(1+\alpha)+K_2'(1\pm\beta)\right)^2} + \frac{(1-\alpha)(1\mp\beta)}{\left(1+K_1'(1-\alpha)+K_2'(1\mp\beta)\right)^2}\right)}{2(1+K_1'+K_2')^{-2}} - 1 \tag{21}$$

Simultaneous and out-of-phase modulation are indicated in Eqn. (21) by the + and - signs, respectively. Plotting Δ in the plane of dimensionless amplitudes for the example case of $K'_1 = 2$ and $K'_2 = 30$ during in and out-of-phase operation results in Figs. 2a and b, respectively. It is useful to assess the results by considering the apparent reaction orders for each reactant given by

$$n_{i,app} = \left(\frac{\partial \ln(r)}{\partial \ln(C_i)}\right)_{C_{i \neq i}}$$
(22)

Application of Eqn. (22) to the LHHW kinetics gives Eqn. (23) for reactants and Eqn. (24) for products

$$n_{i,app} = \frac{1 + (1 - N)K_i' + \sum_{j \neq i}^M K_j'}{1 + \sum_j^M K_j'}$$
(23)

$$n_{i,app} = \frac{-N K_i'}{1 + \sum_{j}^{M} K_j'}$$
 (24)

For this specific case of two components (N=2, $K'_1 = 2$ and $K'_2 = 30$) the apparent orders are estimated from Eqns. (23)-(24) as $n_{1,app} = 0.88$ and $n_{2,app} = -0.81$. It is revealing to consult the schematic plot in Fig. 2c. Two chords are drawn representing two cases with the minimum and maximum values of the modulated concentration being the end points. Modulation at lower concentrations to the left of the rate maximum leads to hindrance while modulation at higher concentrations to the right of the rate maximum leads to enhancement.

Applying the QSS modulation findings for power law kinetics shows that modulation of species B leads to fractional enhancement (n < 0) while modulation of species A leads to hindrance (0 < n < 1). Figs. 2a and b indeed show a region of enhancement at higher dimensionless amplitudes of species B (β) and smaller dimensionless amplitudes of species A (α). However, unlike power law expressions, the largest enhancement does not occur when the convex species has the largest dimensionless amplitude, which in this example occurs when β = 1. Rather, Fig. 2c shows that any modulation with β = 1 hinders the rate as it is impossible to draw a chord anchored at the origin with an average greater than the SS rate curve. This effect is captured in Figs. 2a and b as the enhancement decreases at very high β or α .

In section 2.2, we demonstrated that enhancement during simultaneous modulation with equivalent duty cycles and dimensionless amplitudes ($\alpha = \beta$) is dependent on the sum of apparent reaction orders. For example, in Fig. 1b, when the two individual species are fractional positive order, but the sum of the reaction orders is greater than 1, a region of dynamic enhancement can be observed along the $\alpha = \beta$ axis. Simultaneous modulation of A and B in this Langmuir Hinshelwood case results in negligible enhancement in a region along the diagonal in the β vs. α plane (Fig. 2a). This is a result of the near-zero sum of the apparent reaction orders ($n_{1,app} = 0.88$ and $n_{2,app} = -0.81$). Fig. 2a demonstrates that higher dimensionless amplitudes of species B are required to out-compete the negative effect of a higher dimensionless amplitudes of species A (when β <1). In contrast, out-of-phase modulation of A and B results in a larger region of enhancement (Fig. 2b). During out-of-phase operation (Fig. 2b), the enhancement no longer relies on the sum of apparent orders, and hence enhancement can be observed along the $\alpha = \beta$ axis, unlike the case of in phase operation (Fig. 2a). Individual apparent orders appear to be more important than their sum during out-of-phase operation, resulting in the enlarged region of enhancement in Fig. 2b compared to Fig. 2a.

In section 2.2, we showed that simultaneous modulation may lead to higher rates when the sum of apparent orders is greater than 1. For the case of M total species with N adsorbed and reacting components and L inhibiting products (L+N=M), this translates to the following criteria:

$$\sum_{i=reactants}^{N} n_{i,app} + \sum_{i=products}^{L} n_{i,app} = \frac{N - \sum_{j}^{L} K_{j}'}{1 + \sum_{j}^{M} K_{j}'} > 1 \quad or < 0$$
 (25)

For two adsorbing reactants and no adsorbing products (N=2 and L=0), Eqn. (25) simplifies to Eqn. (26):

$$0 < K_2', 0 < K_1', K_1' + K_2' < 1 \tag{26}$$

The enhancing effect of additive reaction orders for N = 2 only applies when Eqn. (26) is satisfied. These criteria imply that K'_1 and K'_2 must be small enough such that both reactant concentrations are in the positive order regime (to the left of the maximum rate in Fig. 2c) in order to benefit from simultaneous modulation.

For the case of N adsorbing reactants and L inhibiting products, the sum of orders is greater than 1 when the following equation is satisfied:

$$N-1 > \sum_{j=reactants}^{N} K_{j}' + 2 \sum_{j=products}^{L} K_{j}'$$
(27)

This expression shows that more inhibiting products make it more difficult for the sum of the orders to exceed unity, an expected result since apparent orders of inhibiting products are negative. Therefore, to satisfy this criterion it is best for there to be no inhibiting species. Furthermore, the expression shows that if there is one adsorbed reacting component (N=1), it is impossible to exceed an apparent order of 1, which is a characteristic of single order denominator LHHW rate expressions. The second criterion for enhancement during the simultaneous modulation of species is for the sum of apparent orders to be less than zero. This criterion is expressed as the following

$$\sum_{i=n roducts}^{L} K_{j}' > N \tag{28}$$

This expression shows that the sum of apparent orders is less than zero during high degrees of product inhibition relative to the number of reactants. Eqns. (27) and (28) demonstrate that enhancement due to additive reaction orders through simultaneous modulation must occur when reactants fall to the left of the maximum of the rate concentration curve in Fig. 2c (i.e., $n_1 + n_2 + ... > 1$) or when there is extensive product inhibition (i.e. $n_1 + n_2 + ... < 0$). In later sections we will address the implications and effects of QSS operation with LHHW type kinetics in a PFR.

2.4 Simultaneous Modulation for a Bimolecular Reaction in a PFR

As we have seen up to this point, the QSS rate analysis is a simple and informative way of approximating local (differential) rate enhancement. In this section we extend the local QSS analysis to integral operation, i.e. for cases where reactant species concentrations vary along the length of the reactor. We specifically examine reactant feed modulation for the case of the single reaction $A + bB \rightarrow pP$ in an isothermal PFR.

The following reacting species balances account for accumulation, convection, and reaction:

$$\frac{\partial x_A}{\partial \theta} = -\frac{\partial x_A}{\partial \xi} - Da r \tag{29}$$

$$\frac{\partial x_B}{\partial \theta} = -\frac{\partial x_B}{\partial \xi} - b \, Da \, r \tag{30}$$

$$\frac{\partial x_P}{\partial \theta} = -\frac{\partial x_P}{\partial \xi} + p \, Da \, r \tag{31}$$

where

$$r = Da \, x_A^n x_B^m \tag{32}$$

and

$$x_{i} = \frac{C_{i}}{C_{A,Avg}^{f}}; \quad \xi = \frac{z}{L}; \quad \theta = \frac{L}{u_{s}}t; \quad Da = \frac{k\left(C_{A,Avg}^{f}\right)^{n+m-1}L}{u_{s}};$$

The boundary conditions are given by

$$x_{A}(\theta, \xi = 0) = \begin{cases} \left(1 + \alpha_{+}^{f}\right); l \tau \leq \theta < \tau \left(l + s_{A}^{f}\right) \\ \left(1 - \alpha_{-}^{f}\right); \tau \left(l + s_{A}^{f}\right) \leq \theta < \tau \left(l + 1\right) \end{cases}$$
(33)

$$x_{B}(\theta, \xi = 0) = \begin{cases} (1 + \beta_{+}^{f})x_{B,Avg}^{f}; l \tau \leq \theta < \tau \left(l + s_{B}^{f}\right) \\ (1 - \beta_{-}^{f})x_{B,Avg}^{f}; \tau \left(l + s_{B}^{f}\right) \leq \theta < \tau \left(l + 1\right) \end{cases}$$
(34)

where

$$l = 0, 1, 2, ...$$

The initial conditions are given by

$$x_B(\theta = 0, \xi) = x_A(\theta = 0, \xi) = 0$$
 (35)

The system of partial differential equations (PDE's) is solved using the method of lines. For the calculations reported here we discretized the reactor into 20 cells and solved the system of ordinary differential equations in Python using the LSODA algorithm. The fractional enhancement $\Delta(\xi=1)$ was calculated using Eqn. (6) after a cyclic steady state was reached for each cell (very large l). The cyclic average enhancement was compared to the steady state case (i.e., steady state implying $\alpha_+^f = \alpha_-^f = \beta_+^f = \beta_-^f = 0$ in Eqns. (33) and (34)).

The QSS analysis can be applied to integral operation to identify conditions that result in conversion enhancement during periodic operation in a PFR. For illustration, we consider the following combination of reaction orders and stoichiometric coefficients: $n_1 = 0.7$, $n_2 = 0.9$, b = 2, p = 1. We first analyze simultaneous modulation of A and B for which the cyclic average dimensionless feed concentrations of A $(x_{A,Avg}^f)$ and B $(x_{B,Avg}^f)$ satisfy the reaction stoichiometry $(x_{A,Avg}^f = 1)$ and $x_{B,Avg}^f = 2$, with duty cycles $s_A^f = s_B^f = 0.5$ and amplitudes $\alpha^f = \beta^f = 0.9$. According to the QSS analysis, this combination of reaction orders, amplitudes and duty cycles suggest that the local rate will be enhanced since $n_1 + n_2 > 1$. Since Δ varies along the reactor, we calculate the effluent enhancement $\Delta(\xi = 1)$ at cyclic steady state as a function of the Damköhler number (Da). Model predictions in Fig. 3 shows $\Delta(\xi = 1)$ calculated using Eqns. (6), (7) and (8) from earlier. As defined in section 2.1, Eqn. (6) is the exact Δ whereas Eqns. (7) and (8) are approximations of Δ assuming square waves; the former (Eqn. (7)) accounts for differences between cyclic average and SS concentrations, while the latter (Eqn. (8)) assumes they are

equivalent at the reactor outlet. Also shown in the figure are the calculated QSS and SS conversions, X_{OSS} and X_{SS} .

The simulations show the expected monotonically increasing dependence of SS conversion on Da. For the selected reaction orders and stoichiometric parameters, the conversion obtained under modulation leads to integral enhancement for the entire range of Da. The calculated $\Delta(\xi = 1)$ monotonically decreases with Da from a maximum value of 0.42 for Da \rightarrow 0 to -0.2 at Da \sim 4. At $Da\sim0.4$, $\Delta(\xi = 1) = 0$; i.e., enhancement stops. For Da > 0.4, $\Delta(\xi = 1) < 0$ and X_{QSS} approaches X_{SS} . Despite this trend, the QSS operation outperforms SS operation ($X_{QSS}>X_{SS}$) even for conversions greater than 90%.

The deviation between the exact Δ (Eqn. (6)) and estimated Δ (Eqn. (8)) conveys the growing gap between the cyclic average and SS concentrations down the length of the reactor. Specifically, rates are elevated near the inlet of the reactor during QSS operation as result of the additive order effect described in section 2.1. Higher rates in the QSS reactor therefore result in lower cyclic average concentrations relative to SS concentrations at the same Da. Accounting for these differences with Δ approximated using Eqn. (7) gives much better agreement with the exact value obtained from Eqn. (6). This indicates that conversion enhancement is determined both by the degree of reactant modulation as well as difference between cyclic average and steady state concentrations. Specifically, higher SS concentrations relative to the cycle average concentrations along a PFR result in a decreasing Δ as a function of Da as seen in Eqn. (7). In other words, the ratio of the cyclic average and SS concentrations in Eqn. (7) will decrease as Da increases causing Δ to also decrease.

The considered case of a stoichiometric feed with equal dimensionless amplitudes ($\alpha^f = \beta^f$) means that these remain identical along the reactor length, i.e. $\alpha(Da) = \beta(Da)$ for all Da.

This feature is no longer realized if the feed is not stoichiometric and, as a result, the advantage gained through simultaneous reactant modulation when the sum of apparent orders exceeding unity is lost at higher Da. That is, the enhancement diminishes as the local amplitudes are no longer aligned, $\alpha(Da) \neq \beta(Da)$.

To this point, we now consider the case of a non-stoichiometric feed in which B is fed in excess $(x_{A,Avg}^f = 1 \text{ and } x_{B,Avg}^f = 4)$ while all other parameters are kept the same as the earlier stoichiometric case. Fig. 4a shows $\Delta(\xi = 1)$ calculated from Eqns. (6), (7), (8) and (9) defined in section 2.1 along with X_{QSS} and X_{SS} as functions of Da. Comparing Fig. 4a to Fig. 3, as expected, the 5x increase in the B concentration increases the steady state conversion of A for all Da. As for the stoichiometric case, Fig. 4a shows that modulation is beneficial due to the sum of reaction orders exceeding unity. However, the local enhancement decreases with increasing Da, eventually becoming negative. As a result, the gap between QSS and SS diminishes as Da increases. The most significant difference in this case is a much more rapidly decreasing Δ . This is due to the nonstoichiometric feed condition. Fig. 4b shows that dimensionless amplitudes α and β begin to separate from one another, further decreasing the enhancement at the reactor outlet. At $Da \sim 0.3$, $\Delta = 0$ and the rate no longer benefits from QSS operation relative to steady state operation. Although the integral conversion remains higher in the QSS case at $Da \sim 0.3$, it begins to converge towards the SS conversion at this point. It is notable that in the stoichiometric case, α and β remain equivalent hence maintaining the additive order effect which is not the case with nonstoichiometric feeds. Fig. S2.3 in the SI (figure) depicts α and β as a function of Da for the stoichiometric case demonstrating such compositions maintain equivalent dimensionless amplitudes.

Unlike the stoichiometric example, Fig. 4a shows that Δ is more accurately estimated by Eqn. (7) only for Da < 0.6 as it accounts for the difference between the SS and cyclic average concentrations up to $Da \sim 0.6$. However, for Da > 0.6, Eqn. (7) incorrectly predicts an increase in Δ as Da increases. Fig. 4b also shows a reconvergence of α and β after $Da \sim 0.6$. Since both orders have a sum greater than 1, the reconvergence of α and β should improve the rate, hence the increase in Δ predicted by Eqn. (7) in Fig. 4a. However, Fig. 4a shows that Δ (Eqn. (6)) decreases for Da > 0.6, therefore, Eqn. (7) no longer captures the behavior of Δ at higher Da. Rather, the solution can be found in Figs. 4c and d which plot x_A and x_B as functions of dimensionless time (θ) before (at Da = 0.5) and after (at Da = 0.9) the point, $Da \sim 0.6$. Fig. 4c shows that for Da = 0.5, the concentration waves remain in-phase, resulting in a positive effect on the fractional enhancement as previously described. However, Fig. 4d shows that after $Da \sim 0.6$ (at Da = 0.9), the concentration waves are no longer in-phase with one another. This implies that the concentration wave undergoes a phase change relative to its initial wave form which occurs at $Da \sim 0.6$, resulting in further enhancement losses. Specifically, the concentration wave of species A inverts over the x_i axis from Figs. 4c to d. This results in a wave that is out of phase with its inlet waveform.

A similar effect of concentration wave inversion was reported by Marin *et. al.* in the case of carbon monoxide (CO) oxidation on Pt catalysts. In some instances, their simulations predicted bulk phase oxygen and CO concentration waves entering the reactor out-of-phase and exiting approximately in-phase [7]. In our case, since the waves are no longer in-phase, the rate no longer benefits from the combined reaction orders and instead suffers from the individual fractional orders. Eqn. (9) in Fig. 4a solves for Δ during out-of-phase operation accounting for differences in SS and cyclic average concentrations. The trajectory of Eqn. (9) more closely follows that of Δ (Eqn. (6)) for Da > 0.6. Although Eqn. (9) follows the trajectory of Eqn. (6), deviations between

equations arise from the distortions of the square waves which is shown by x_A in Fig. 4d as this negates the assumption of square concentration waves.

It is important to note that the wave phase change phenomenon is not a result of waves shifting past each other. Rather, it is a result of disproportionate decreases in the concentration wave maxima and minima values. Both A and B are consumed along the length of the reactor to produce P. The positive reaction orders for A and B also indicate that they will react at higher rates during the concentration wave maxima relative to the minima. This coupled with the non-stoichiometric feed results in a disproportionate decrease of the concentration wave maxima and minima. This disproportionate decrease results in the maxima of the limiting reactant (A) eventually falling below its minima generating a wave that is out-of-phase with reactant B and its (A's) inlet waveform. Therefore, this effect is more accurately referred to as a wave inversion rather than a phase change.

It is possible to determine the location at which a wave inversion occurs for a nonstoichiometric feed. For example, if the maxima of the concentration continuously decreases past the minima as Da increases; the point after which the waves become out-of-phase occurs at the Da when both the maxima and minima are equal. The point of wave inversion for species i occurs at the Da when $x_{i,Max}(Da) = x_{i,Min}(Da)$. The Da at which this occurs can be determined by solving the SS model with inlet boundary conditions equivalent to the concentration wave maxima and minima and finding the Da at which the solutions intersect. This is demonstrated in Fig. 4e which shows the intersection between the limiting reactant (A) steady state maxima and minima solutions $(x_{A,Max}(Da) = x_{A,Min}(Da))$ occurring at $Da \sim 0.6$. This is illustrated in Fig.4a as the point where the in-phase operation assumption (Eqns. (7)) breaks down and the

concentration waves switch from in to out-of-phase modulation, hence the better prediction by Eqn. (9).

In summary, this analysis provides a useful method of selecting inlet conditions for square waves during QSS dynamic operation. Differences in the cyclic average from steady state reactant concentrations, wave inversion and distortion at different Da result in inaccurate predictions during high conversion integral behavior. Despite the lack of accuracy, overall conversions during QSS operation remain higher than steady state operation even above 90% SS conversion. Later sections apply the method to predict wave inversion to the periodic operation of ethane and oxygen during oxidative dehydrogenation to ethylene.

2.5 Simultaneous Modulation for a Single Reaction in a PFR LHHW Kinetics

Here we extend the integral analysis to a reaction having LHHW kinetics. We consider LHHW kinetics involving self-inhibition by two components as follows:

$$A + * \rightarrow A *$$

$$B + * \rightarrow B *$$

$$A * + B * \rightarrow P + 2 *$$

The rate under surface reaction control is given by

$$r = \frac{L}{C_{A,Avg}^{f} u_{s}} \frac{k_{3} K_{A}' K_{B}' x_{A} x_{B}}{(1 + K_{A}' x_{A} + K_{B}' x_{B})^{2}}$$
(36)

where

$$K'_{i} = C^{f}_{A,Avg}K_{i}; D\alpha = \frac{L}{C^{f}_{A,Avg}u_{s}} \frac{k_{3}K'_{A}K'_{B}x^{f}_{B,Avg}}{\left(1 + K'_{A} + K'_{B}x^{f}_{B,Avg}\right)^{2}}$$

The computed results for Δ , X_{QSS} and X_{SS} as functions of Da in a PFR subject to a stoichiometric feed ($x_{A,Avg}^f = 1$ and $x_{B,Avg}^f = 1$) with $K_A' = 2$, $K_B' = 30$, $s_A^f = s_B^f = 0.5$, $\alpha^f = 1$

 $0.1 \text{ and } \beta^f = 0.5 \text{ during simultaneous modulation are plotted in Fig. 5a. Dimensionless}$ amplitudes α^f and β^f were selected from Fig. 2a as they result in a positive Δ while a stoichiometric feed was used to prevent concentration wave inversion. As shown in Fig. 5a, the fractional enhancement (Δ) steadily increases to a maximum before rapidly dropping. This behavior is understood by considering the rate versus concentration curve in Fig. 2c which reaches a maximum rate at an intermediate concentration value. As the reaction proceeds down the reactor, the concentration minima will rise to the maximum of the rate curve in Fig. 2c shown by the red dashed chord, before falling rapidly, resulting in rate hinderance as illustrated by the purple line in Fig. 2c. Thus, the initial rise of the rate enhancement in Fig. 5a (Da<0.25) is a result of the concentration wave minima approaching the rate versus concentration maximum. The rapid decrease at (Da > 0.25) is a result of the minima falling to the left of the rate maxima on the rate versus concentration plot. It is important to note that the QSS rate will be hindered if the concentration wave maxima and minima remain to the right and left of the rate versus concentration maximum in Fig. 2c respectively. If the concentration maximum and minimum both fall to the left of the rate versus concentration curve maximum, periodic operation will have no effect on the rate due to the apparent first order nature of this regime. In the following paragraph we discuss the importance of apparent reaction orders on QSS operation of LHHW reactions.

The point of maximum enhancement as a function of Da for a LHHW rate expression can be determined from the apparent reaction orders at the maximum and minimum concentrations of a modulating feed. The rate dependence on concentration for a rate expression having a second order denominator transitions from a positive to negative reaction order at the rate versus concentration maximum (Fig. 2c). As a result, the Da value at which the apparent reaction order for the minimum concentration transitions from negative to positive represents the maximum Δ as

a function of Da in Fig. 5a. The criteria for maximum Δ as a function of Da can therefore be noted as when $n_{i,max} < 0$ and $n_{i,min} = 0$. This implies that enhancement begins to decrease when the apparent orders of the maxima and minima are less than and greater than zero, respectively $(n_{i,max} < 0 \text{ and } n_{i,min} > 0)$. Fig. 5b shows the apparent reaction orders at the concentration wave maxima and minima as functions of Da using the steady state model with feed conditions set to the concentration wave maxima and minima concentrations. Apparent reaction orders of species A at the maxima $(n_{A,max})$ and minima $(n_{A,min})$ are both positive and therefore lie to the left of the rate versus concentration curve maxima. This, coupled with the linear dependence of rate on concentration to the left of the rate maxima in Fig. 2c, suggests that modulation of A alone does not significantly affect the rate. This is further confirmed in Fig. 5b as $n_{A,max}$ and $n_{A,min}$ are both close to 1 for small Da (Da < 0.2). However, Fig. 5b shows that $n_{B,max}$ and $n_{B,min}$ are both negative until a Da slightly higher than 0.25, at which point n_{B,min} becomes positive. When n_{B,max} and n_{B,min} < 0, the rate is enhanced through QSS operation. As the reaction proceeds to higher Da, $x_{B,min}$ will eventually fall to the left of the rate maxima (Fig. 2c) while x_{B,max} remains to the right. This criterion can be mathematically written as the Da when

$$n_{i,Min}(Da) = 0 \text{ and } n_{i,Max}(Da) < 0$$
 (37)

In section 2.2 we considered the effects of dimensionless feed amplitudes (α^f and β^f) on the maximum Δ . There we showed that enhancement is dependent on the sum of apparent reaction orders for the case when reactants A and B have equivalent dimensionless amplitudes and duty cycles. Fig. 5b shows that at Da < 0.25 species A and B have positive and negative reaction orders, respectively. Therefore, simultaneous modulation of A and B with equivalent duty cycles and dimensionless amplitudes will decrease Δ as a result of the positive apparent order of A hindering the enhancing effects of the negative apparent order from species B. Therefore, the ideal conditions

for QSS operation involves $\alpha^f = 0$ and $0 < \beta^f < 1$. Fig. 6c plots Δ as a function of Da for various α^f where $\beta^f = 0.5$. Fig. 6c shows that the maximum Δ decreases in the limit of $\alpha^f \to \beta^f$. As the dimensionless amplitudes $(\alpha^f \text{ and } \beta^f)$ become equivalent, the enhancing effects of the negative apparent order of B are overcome by the positive apparent order of species A. Furthermore, Fig. 2a showed that Δ decreases as $\alpha^f \to \beta^f$. Therefore, the QSS rate analysis described in section 2.3 is an effective method of determining optimal periodic feed conditions that result in maximum rate enhancement for LHHW kinetics in a PFR.

Similar to the point of wave inversion, the Da at which the minimum of the concentration wave reaches the rate maxima can be used to identify operational parameters when using LHHW kinetics that have a maximum rate. The wave inversion and maximum enhancement points indicate the regions at which the rates begin to lose enhancement during QSS operation. Furthermore, these points can be determined by solving the steady state balances at the concentration wave maxima and minima which may significantly reduce computational time needed to determine when the phenomena will occur.

2.6 Simultaneous Modulation for Reactions in Series in a CSTR

In this section, we will extend the QSS analysis to study the effects of simultaneous modulation in a CSTR involving consecutive reactions. Lee and Bailey studied the effects of simultaneous bang-bang reactant modulation on the yield of an intermediate product P₁ as described by the following reaction scheme [13]:

$$A + B \rightarrow P_1$$

$$B + P_1 \rightarrow P_2$$

The resulting non-dimensional CSTR species balances are as follows [13]:

$$\frac{dx_A}{d\theta} = x_A^f - x_A - r_1 \tag{38}$$

$$\frac{dx_B}{d\theta} = x_B^f - x_B - r_1 - r_2 \tag{39}$$

$$\frac{dx_{P_1}}{d\theta} = x_{P_1} + r_1 - r_2 \tag{40}$$

$$\frac{dx_{P_2}}{d\theta} = x_{P_2} + r_2 \tag{41}$$

The non-dimensional rate terms are given by:

$$r_1 = Da_1 x_A x_B \tag{42}$$

$$r_2 = Da_2 x_B x_{P_1} \tag{43}$$

with the following dimensionless parameters

$$x_i = \frac{C_i}{C_{A,Avg}^f}; \quad \theta = \frac{F}{V}t; \quad Da_i = \frac{k_i V C_{A,Avg}^f}{F}; \quad l = 0,1,2 \dots$$

The feed concentrations of A and B are given by,

$$x_A^f(\theta) = \begin{cases} (1 + \alpha_+^f); l \ \tau \le \theta < \tau \left(l + s_A^f\right) \\ 0; \tau \left(l + s_A^f\right) \le \theta < \tau \left(l + 1\right) \end{cases} \tag{44}$$

$$x_{B}^{f}(\theta) = \begin{cases} \left(1 + \beta_{+}^{f}\right) x_{B,Avg}^{f}; l \tau \leq \theta < \tau \left(l + s_{B}^{f}\right) \\ 0; \tau \left(l + s_{B}^{f}\right) \leq \theta < \tau \left(l + 1\right) \end{cases}$$

$$(45)$$

The model was solved here using the LSODA algorithm in Python. Fractional rate enhancements were determined by numerically integrating the rate as a function of dimensionless time after the system reached a cyclic steady state. Similar to Lee and Bailey [13], data at higher conversions of A were achieved by increasing the average inlet concentration of B while maintaining a constant residence time and inlet concentration of A.

Lee and Bailey [13] noted a significant increase in P₁ yield during the simultaneous modulation of species A and B shown in a reconstruction of their work in Fig. 6a. In contrast, the individual modulation of species B hinders the rate at higher conversion of A. At first glance, the

first order rate dependency of A and B indicates that any individual modulation of either component should not have any effect on r_1 . This is indeed observed in Fig. 6b at conversions of A less than 25% for the individual modulation of B. However, Eqn. (19) suggests the simultaneous modulation of A and B should enhance the rate of P_1 formation as the orders have a sum greater than 1. This effect is indeed observed in Figs. 6a and b by the larger P_1 yields and r_1 formation rate enhancement, respectively, when modulating A and B simultaneously.

At conversions below 10%, effects from the undesired reaction (r_2) can be ignored as there is less P_1 present. However, as the conversion and therefore concentration of P_1 begins to increase, it becomes necessary to consider the impact of the second reaction. At higher A conversion a higher yield of P₁ is obtained (Fig. 6a). This impacts the overall dynamic enhancement as P₁ further reacts with B to produce the undesired product P₂. The first order dependencies of reactants A and B on the P₁ formation rate indicate that the rate and therefore P₁ concentration will increase with increasing reactant concentrations. This effect results in a P₁ concentration wave that modulates in-phase (simultaneously) with reactants A and B at the outlet of the CSTR as illustrated in Figs. 6c and d. Coupling this with the fact that the CSTR rate depends on the outlet concentrations, the resulting simultaneous modulating concentration waves of P₁ and B begin to enhance the P₂ formation rate. This effect is observed in both the simultaneous and single species modulation cases, especially at higher A conversion, as seen in Fig. 6b. Therefore, the individual modulation of species B does not enhance r₁ but results in an in-phase cyclic profile of P₁ which enhances r₂ hence decreasing P₁ production and increasing its consumption. Simultaneous modulation of A and B is able to outperform this by enhancing the production of P₁ rather than just improving its consumption.

As demonstrated, the QSS local dynamic rate analysis provides a suitable method to identify regions of dynamic operation that induce yield enhancements in a CSTR with reactions in series. While the accuracy of the method presented is limited to lower conversions, concepts such as additive reaction orders through simultaneous modulation offer insights into the effects of dynamic operation on processes with multiple reactions at higher conversion.

2.7 Model Validation: Ethane Total Oxidation Over Spinel Catalysts

We experimentally evaluated the application of QSS analysis methods for the total oxidation of ethane over a supported NiCo₂O₄ spinel catalyst (CDTi). The fractional rate enhancements for CO₂ formation during square wave and SS operation are compared for different reactor feed amplitudes, phase shifts and duty cycles. The enhancement expressions in Eqn. (6) were used to integrate the data and Eqn. (7) was used to generate the theoretical curve. Experimental conditions and details are listed in SI 5.3.

The simultaneous QSS modulation experiment was conducted by testing various dimensionless amplitudes along the curve $\beta=1$ - α . As shown in Fig. 7a, the experimental CO₂ formation rate enhancement closely follows the model prediction using Eqn. (7). As described earlier, the rate during simultaneous modulation of two reactants described by power law kinetics will behave as a single reactant whose order is the sum of the individual orders. With the fractional orders of C₂H₆ and O₂ being 0.22 and 0.48, respectively, that order is 0.70 with the dimensionless amplitudes given by $\alpha = \beta = 0.5$ and equal duty cycles. With the combined order being less than unity, the QSS dynamic operation results in dynamic hindrance. Since 0.7 is closer to 1, the fractional enhancement moves closer to 0 when $\alpha = \beta = 0.5$. In other words, the steady state rate versus concentration curve becomes more linear for the combined species with an order of 0.7. It is noted that the data point at $\alpha = 1$ was determined by assuming that no CO₂ was formed at the

rate minima due to the power law rate dependency (i.e., if the O_2 concentration is zero, so is the rate). At α =1, the oxygen concentration oscillates between 0 and 1.75% but the CO_2 formation rate did not approach zero in the absence of oxygen. As in the absence of gaseous oxygen, C_2H_6 is still able to react with oxygen stored on the spinel catalyst which does not reach a steady state until the catalyst is stripped of O_2 . Total reduction requires a very large period and afterwards the catalyst is unable to return to its initial state. Therefore, the data point is obtained by multiplying the duty cycle by the rate at the O_2 concentration maxima.

Further validation of the theory for out-of-phase periodic operation was conducted using Eqn. (10). Fig. 7b compares the experimental results and model predictions along the curve $\alpha = \beta$. As described earlier, out-of-phase operation during QSS operation will only exhibit enhancement if the individual orders are either greater than 1 or less than 0. In this case, neither of these criteria are satisfied and therefore there is no enhancement. Instead, as the components are modulated to a higher degree (increasing α and β), the rate becomes further hindered due to the fractional reactant orders.

A third validation was conducted by examining the effect of duty cycle on the fractional enhancement. The effects of QSS operation become more exaggerated at lower duty cycles as was previously discussed. Fig. 7c shows that the fractional enhancement increases with increasing duty cycle. Again, this shows that the dynamic effects of QSS operation will become more prominent as the wave maximum approaches a delta function. As previously discussed, the wave maxima is shifted along the rate versus concentration curve to preserve equivalent cyclic averages during changes in the duty cycle. This shift in the maxima results in a decrease of the cyclic average rate that is achieved with higher duty cycles like the effects shown in SI 3.1.

In summary, the QSS model shows quantitative agreement with catalytic ethane total oxidation data collected at low conversions. Effects of different dimensionless amplitudes, duty cycles, and phase shifts are all captured by the QSS analysis. In the following section we demonstrate an experimental case of concentration wave inversion.

2.8 Concentration Wave Inversion: Ethane Oxidative Dehydrogenation

In section 2.4, we discussed the phenomena of concentration wave inversion and how to predict when it will occur using SS conservation equations. In this section, we experimentally demonstrate concentration wave inversion during the oxidative dehydrogenation of ethane to ethylene over a 7 wt% MoO₃/Al₂O₃ catalyst. A simple triangular reaction network for ethane ODH is depicted as follows

$$C_2H_6 + O_2$$
 $T_1=1.8*10^{-1}[C_2H_6]$
 $T_2=1.21*10^{-2}[C_2H_6]$
 $T_3=2.3*10^{-1}[C_2H_4][O_2]^{0.26}$

Schematic 1: Reaction pathways during the oxidative dehydrogenation of ethane to ethylene and associated power law rate expressions with estimated kinetic parameters. Rates above are reported in [µmol/mg-cat/min]. Details on experiments, synthesis and conditions are located in SI 5.4.

Kinetic parameters for each reaction in scheme 1 were obtained through an integral fitting of SS data and used to plot the O_2 concentration wave maxima and minima as functions of W/F in Fig. 8. Fig. 8 shows that the O_2 concentration maxima and minima intersect at W/F = 2.8 mg sccm⁻¹. As introduced in section 2.4, the intersection between the SS maxima and minima concentration profiles denotes the point of wave inversion. Therefore, Fig. 8 suggests that the O_2 concentration wave during periodic operation under the same conditions will become out of phase with its initial waveform at W/F \sim 2.8 mg sccm⁻¹. The point of wave inversion was verified by monitoring the concentration profiles of C_2H_6 , O_2 , C_2H_4 and CO_2 as functions of time at the effluent of reactors

with different W/F which are shown in Figs. 9a-d. Fig. 9a shows the concentration wave just before it enters the MoO₃ catalyst bed. C₂H₆ and O₂ are oscillated in phase implying the concentration waves reach a maxima and minima at the same times. The blue arrow indicates the C₂H₆ and O₂ concentration wave maxima. Fig. 9b shows the effluent concentration of C₂H₆, O₂, C₂H₄ and CO₂ versus time for W/F = 2.1 mg sccm^{-1} . At higher residence times, O_2 and C_2H_6 are consumed, resulting in the decreasing cyclic average observed in Fig. 9b. The O₂ maxima indicated by the blue arrow (~1.8*10⁴ ppm) in Fig. 9b is much closer to its effluent minima (~1.6*10⁴ ppm), implying that O₂ is being consumed more rapidly at its maxima relative to its minima. Fig. 9c shows that the effluent O₂ concentration maxima (1.7*10⁴ ppm) indicated by the blue arrow is almost equivalent to its minima $(1.6*10^4 \text{ ppm})$ for W/F = 2.6 mg sccm⁻¹ which is similar to the point of wave inversion in Fig. 8. The equivalence between O2 concentration wave maxima and minima implies that the wave inverts 180° from its original phase and that any further reaction (higher W/F) will result in an O₂ concentration wave that is no longer in-phase with its original wave form. Fig. 9d shows that the original O₂ concentration maxima (1.5*10⁴ ppm) indicated by the blue arrow is now less than the original concentration wave minima (1.6*10⁴ ppm) at a W/F of 3.2 mg sccm⁻¹. At this W/F value the O₂ concentration wave is now 180° out of phase with its inlet wave form. It is important to note that Fig. 9a shows the O₂ and C₂H₆ concentration waves enter the reactor in phase but exit the reactor out-of-phase in Fig. 9d (for W/F=3.2mg sccm⁻¹). More importantly, SS solutions plotted in Fig. 8 are able to accurately determine the point of wave inversion found in Fig. 9c which occurs at W/F ~ 2.8 mg sccm⁻¹. Here, we have experimentally demonstrated that the application of SS conservation equations to concentration wave maxima and minima may be used to determine the point of wave inversion in a PFR during C₂H₆ ODH.

2.9 Maximum Rate Enhancement: Methane Oxidation

In this section, we will apply the QSS rate analysis to methane oxidation over Platinum Group Metals (PGM) catalyst which exhibit similar LHHW rate versus concentration dependencies as those found in section 2.5. Work by Karinshak et. al. found that modulating oxygen during total oxidation of methane on a Pt/Pd catalyst resulted in lower light off temperatures compared to SS operation [30]. The modulation frequency of these experiments was low enough permitting the use of the QSS approach described in this paper. The effect of amplitude on light off temperature during QSS operation of methane oxidation is plotted in fig. 10a. As illustrated in their work, increasing the oxygen amplitude while maintaining an equivalent cyclic average resulted in decreasing light off temperatures until the amplitude exceeded 0.028 as shown in Fig. 10a [30]. The decreasing light off temperature is the result of the QSS rate being enhanced by modulation within the negative order regime of the rate versus concentration curve illustrated in Fig. 10b. Fig. 10a demonstrates that upon increasing the amplitude beyond 0.028, the light-off temperature began to shift towards the SS light off temperature-[30]. The reconvergence of QSS and SS light off temperatures are a consequence of the concentration minima falling to the left of the rate maxima as detailed in section 2.5 and illustrated in Fig. 10b. It is important to note that strong oxygen inhibition over PGM catalysts may result in isothermal multiplicity of the SS rate as shown by Ratcliff et. al. [31]. However, during experiments conducted by Karinshak, the amplitude was large enough such that the maxima and minima rates fell on the single valued curve described by fig. 10b [30]. This section highlights the agreement between the QSS theory presented in this publication to experimental observations during methane oxidation with LHHW kinetic behavior.

3. Conclusions

In this paper we have developed a simple method to estimate the effects of multiple dynamically fed reactants during QSS isothermal operation on reaction rates. Fractional rate enhancement is shown to be a function of reactant dimensionless amplitudes, duty cycles and reaction orders. Differences in rates when subject to modulating reactant concentrations compared to SS can be attributed to disproportionate scaling of the rate maxima and minima. Multi reactant modulation follows similar trends to single reactant modulation except in the case of in-phase operation. If multiple reactants are modulated simultaneously while sharing equivalent duty cycles and dimensionless amplitudes, the rate will behave as if it were dependent upon one species whose order is the sum of the individual reactants. This effect may lead to enhancement in the cases when the orders sum outside the range 0-1. The analysis can used to determine inlet dynamic parameters for QSS operation of both a PFR and a CSTR. Analysis accuracy is reduced at higher reactant conversions due to differences in the cyclic average and SS concentrations, wave phase inversion and wave distortion. Regardless of these limitations, effects predicted by the QSS rate analysis persist to relatively high conversions. Dynamic effects on more complex reaction schemes such as reactions in series can also be explained through the results of the QSS analysis. For example, the exaggerated effects resulting from smaller duty cycles and simultaneous reactant modulation are both captured by the analysis. Experiments involving dynamic operation of alkane oxidation demonstrate good agreement with theoretical predictions of the fractional rate enhancement, point of concentration wave inversion and maximum rate enhancement. Future work will include extension of the analysis to non-isothermal QSS operation and systems subject to multiple distributed dynamic feeds and more complex reaction networks.

Acknowledgements

The authors acknowledge support from the National Science Foundation (EFMA 2029359). We also acknowledge the spinel catalyst provided by CDTI (Oxnard, CA).

Symbols

A = Reactant A

B = Reactant B

C_{i, Avg} = Cyclic Average Concentration of species i

 C_i = Concentration of species i

 C_{+} = Concentration wave maximum

C₋= Concentration wave minimum

Da = Damköhler Number

F = Volumetric flow rate

1 = Counter for periodic concentration profiles (i.e. 1=0,1,2,3...)

 P_i = Product number i

 k_{eff} = Reaction rate constant

 K_i = Equilibrium adsorption constant of species i

 K_{i} ' = equilibrium adsorption constant multiplied by the cyclic average of species i $(C_{i, \text{Avg}} * K_{i})$

 n_i (or m_i) = Power law reaction orders of species i

r = reaction rate

s = Duty cycle/ fraction of period when the concentration wave is at a maximum

t = Time

 u_s = Superficial velocity

V = Volume of reactor

 x_i = Dimensionless concentration of species i (normalized by the cyclic average of the limiting reactant)

Greek symbols

 α = Dimensionless amplitude of species i (or A)

 β = Dimensionless amplitude of reactant B

 ξ = Dimensionless distance (z/L)

 γ = Dimensionless amplitude of species modulating out-of-phase (from those with dimensionless amplitude alpha)

 θ = Dimensionless time (= $\frac{L t}{u_s}$ for a PFR) and (= $\frac{F t}{V}$ for a CSTR)

 Δ = Fractional rate enhancement

 τ = Period of oscillation

Subscripts

Avg = Cyclic Average (Integral Average)

QSS = Quasi Steady State

SS = Steady State

+ = At the concentration wave maximum

- = At the concentration wave minimum

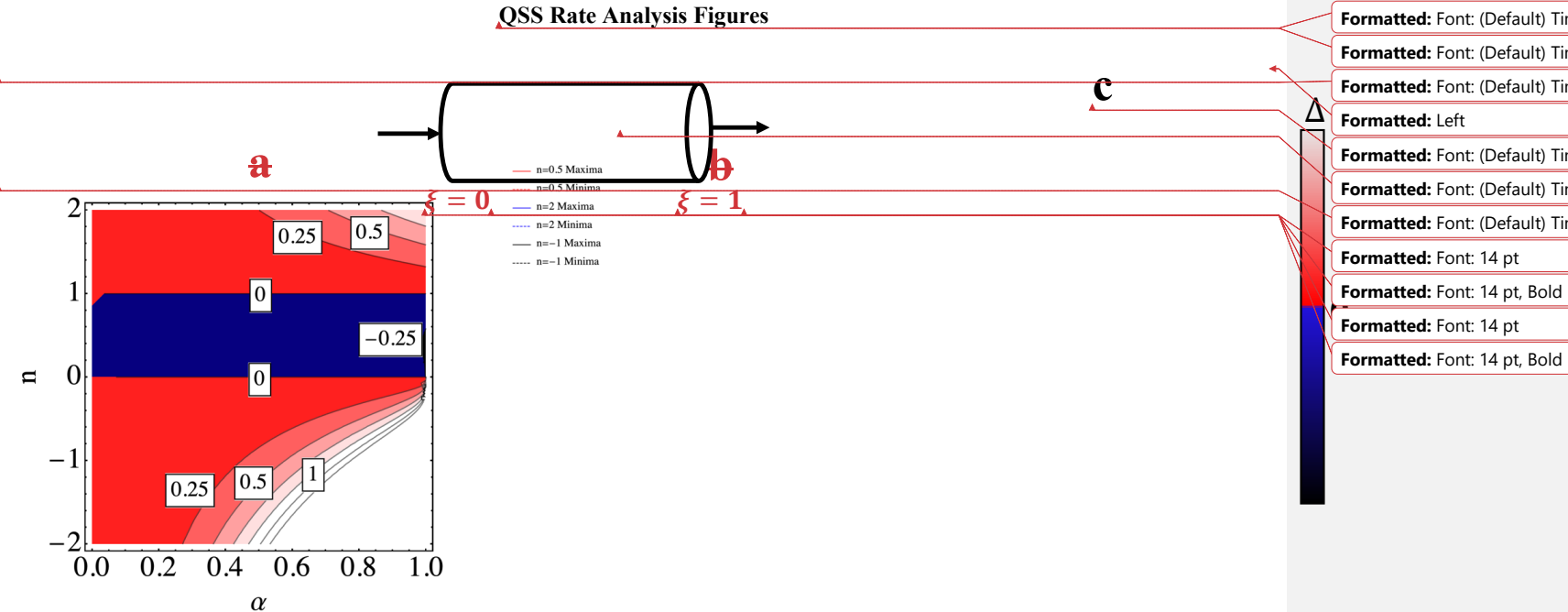
Superscripts

f = Feed (at entrance of the reactor)

References

- [1] Silveston, P. L. Sadhana 10, 217–246 (1987).
- [2] Silveston, P. L., Hudgins, R. R. & Renken, A. Catal. Today 25, 91–112 (1995).
- [3] Silveston, P. L. & Hudgins, R. R. *Periodic Operation of Chemical Reactors*. (Elsevier Science, 2013).
- [4] Huang, X.-F., Li, C.-Y., Chen, B.-H., & Silveston, P. L. AIChE J. 48, 846–855 (2002).
- [5] Mcneil, M. A., & Rinker, R. G. Chem. Eng. Commun. 127, 137–149 (1994).
- [6] Schuurman, Y., & Gleaves, J. T. Cat. Today 33, 25–37 (1997).
- [7] Lie, A. B. K., Hoebink, J. & Marin, G. B. Chem. Eng. J. Biochem. Eng. J. 53, 47–54 (1993).
- [8] Grabmüller, H., Hoffmann, U. & Schädlich, K. Chem. Eng. Sci. 40, 951–960 (1985).
- [9] Hoffmann, U. & Schädlich, H. K. Chem. Eng. Sci. 41, 2733–2738 (1986).
- [10] Marin G. B., Safety and Environment Monolith Reactors (2014).
- [11] Cho, B. K. Ind. Eng. Chem. Fundam. 22, 410–420 (1983).
- [12] Bailey, J. E., & Sinčić, D. IFAC Proceedings Volumes 11, 2071–2077 (1978).
- [13] Lee, C. K. & Bailey, J. E. Ind. & Eng. Chem. Process Des. and Dev. 160–166 (1980).
- [14] Gottlieb, K., Schädlich, H.-K & Hoffmann, U. Chemie. Ing. Tech. 55, 963–965 (1983).
- [15] Horn, F. J. M., & Lin, R. C. Ind. & Eng. Chem. Process Des. and Dev., 6, (1967).
- [16] Horn, F. J. M., & Bailey, J. E. J. of Opt. Theory and App., 2, (1986).
- [17] Sinčić, D. & Bailey, J. E. Chem. Eng. Sci. 35, 1153–1161 (1980).
- [18] Sterman, L. E. & Erik Ydstie, B. Chem. Eng. Sci. 45, 721–736 (1990).
- [19] Thullie, J., Chiao, L., & Rinker, R. G. Chem. Eng. Sci. 42, 1095–1101 (1987).
- [20] Parulekar, S. J., & Lee, J. Chem. Eng. Sci. 48, 3007–3035 (1993).
- [21] Zuyev, A., Seidel-Morgenstern, A. & Benner, P. Chem. Eng. Sci. 161, 206–214 (2017).
- [22] Petkovska, M., Nikolić, D. & Seidel-Morgenstern, A. Isr. J. Chem. 58, 663-681 (2018).

- [23] Nikolić, D., Seidel-Morgenstern, A., & Petkovska, M. Chem. Eng. And Tech. 39, (2016).
- [24] Felischak, M., Kaps, L., Hamel, C., Nikolic, D., Petkovska, M., & Seidel-Morgenstern, A. *Chem. Eng. J.* 410 (2021).
- [25] Douglas, J. M., & Rippin, D. W. T. Chem. Eng. Sci., 21, (1966).
- [26] Gutsche, R., Lange, R., & Witt, W. Chem. Eng. Sci., 58, (2003).
- [27] Urmès, C. et al. Chem. Eng. Sci. 214, 114544 (2020).
- [28] Novotný, P., Yusuf, S., Li, F., & Lamb, H. H. J. Chem. Phys. 152, 044713 (2020).
- [29] Novotný, P., Yusuf, S., Li, F., & Lamb, H. H. Catal. Today, 317, 50–55 (2018).
- [30] Kang, S. B., Karinshak, K., Chen, P. W., Golden, S., & Harold, M. P. Catal. Today, **360**, 284–293 (2021).
- [31] Ratcliff, J., Karinshak, K., & Harold, M. P. Chem. Eng. Sci. (in review).



Formatted: Font: (Default) Times New Roman Formatted: Font: (Default) Times New Roman Formatted: Font: (Default) Times New Roman **△** Formatted: Left Formatted: Font: (Default) Times New Roman Formatted: Font: (Default) Times New Roman Formatted: Font: (Default) Times New Roman Formatted: Font: 14 pt Formatted: Font: 14 pt, Bold Formatted: Font: 14 pt

Formatted: Right: 0.25"

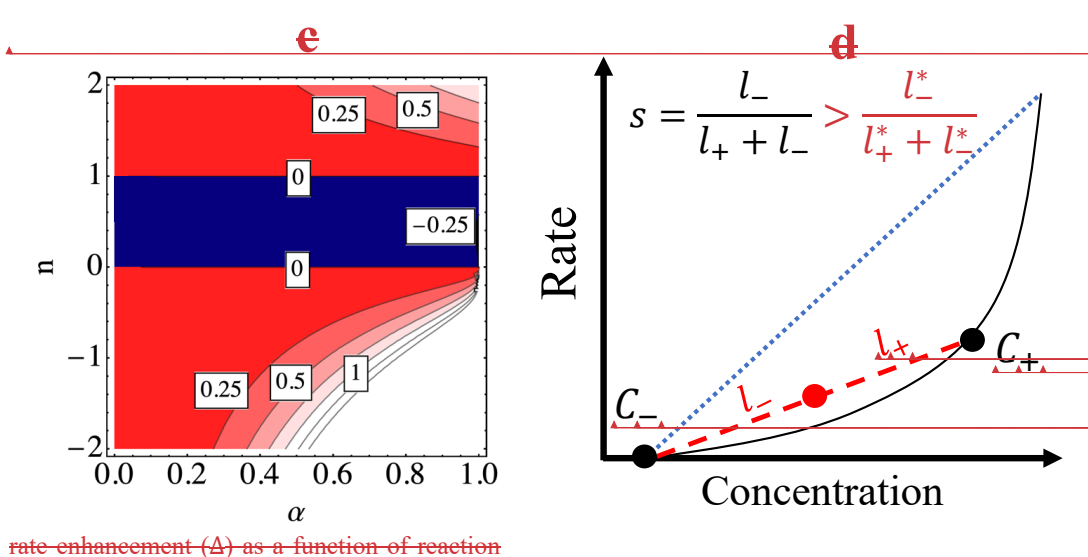


Figure 1: (a) Fractional rate enhancement (A) plotted amplitude (a) and reaction order (n) for a 50% duty cycle at a 50% duty cycle (s=0.5) of by the steady state rate for reaction orders of 0.5 (___), 2 (<u></u> and 1 (<u>)</u>. (c) Fractional order and duty eyele at α_{-} = 0.5. (d) Rate versus concentration for a power law rate expression with an apparent order greater than [1]. I

Formatted: Font: (Default) Times New Roman

Commented [AM1]: Considering moving unimolecular section to supplemental which would also move figs. 1b-d to supplemental.

Formatted: Justified

Formatted: Font color: Red

Formatted: Font color: Red

Formatted: Font color: Red

Formatted: Font color: Text 1

Commented [HMP2]: The figure is confusing. The three points for the dashed case are shown. Shouldn't points also be shown for the dotted case?

Commented [AM3R2]: Added points to fig. 1d

Formatted: Justified, Line spacing: single

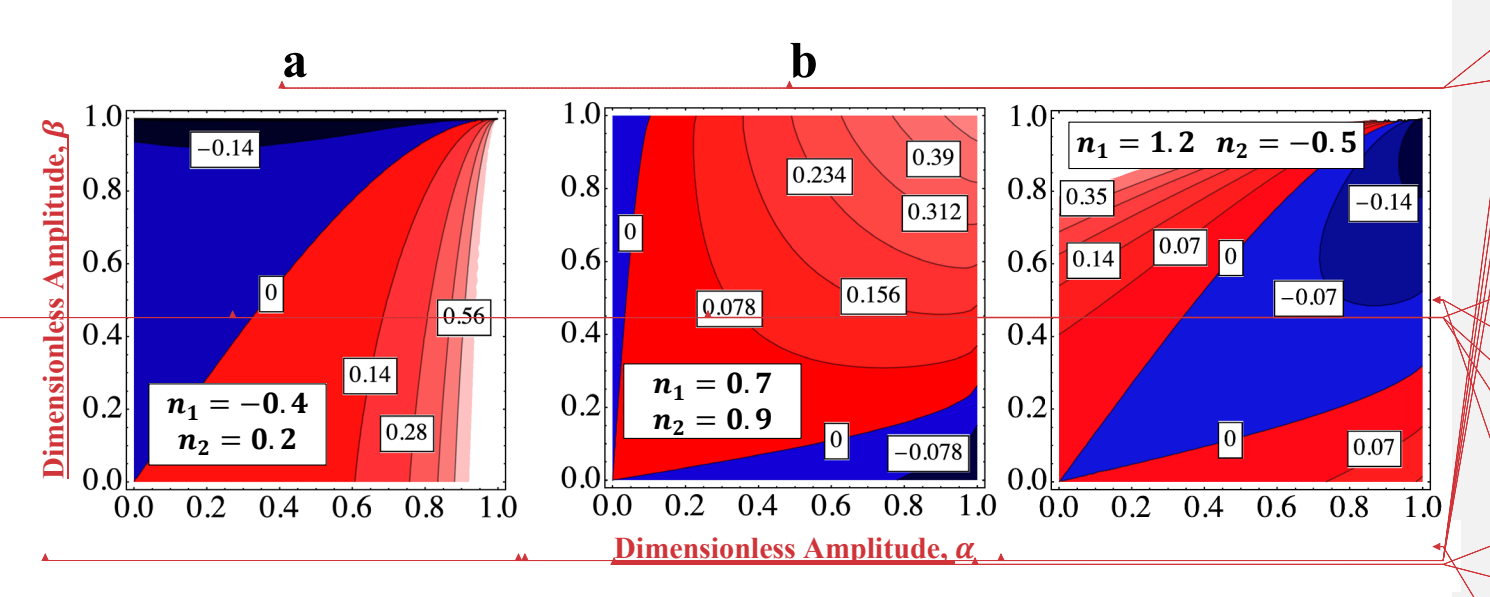


Figure 21: Local fractional rate enhancement with respect to dimensionless amplitudes of species 1 (α) and 2 (β) for the following combinations of reaction orders for simultaneous modulation (a) $n_1 + n_2 < 1$, $n_1 < 0 < n_2 < 1$; (b) $n_1 + n_2 > 1$, $0 < n_1 & n_2 < 1$; (c) $0 < n_1 + n_2 < 1$, $n_2 < 0 & n_1 > 1$.

Fractional rate enhancement with respect to dimensionless amplitudes of species 1 (α) and 2 (β) for the following combinations of reaction orders for simultaneous modulation (a) $n_1 + n_2 < 1$, $n_1 < 0 < n_2 < 1$; (b) $n_1 + n_2 > 1$, $0 < n_1 & n_2 < 1$; (c) $n_1 + n_2 < 1$, $n_2 < 0 & n_3 > 1$.

Formatted: Font: (Default) Times New Roman

Formatted: Font: (Default) Times New Roman, 14 pt

Formatted: Centered

Formatted: Font: Bold

Formatted: Font: (Default) Times New Roman, 14 pt,

Formatted: Centered

Formatted: Font: Bold

Formatted: Font: (Default) Times New Roman, 14 pt,

Bold

Bold

Formatted: Centered

Formatted: Font: (Default) Times New Roman

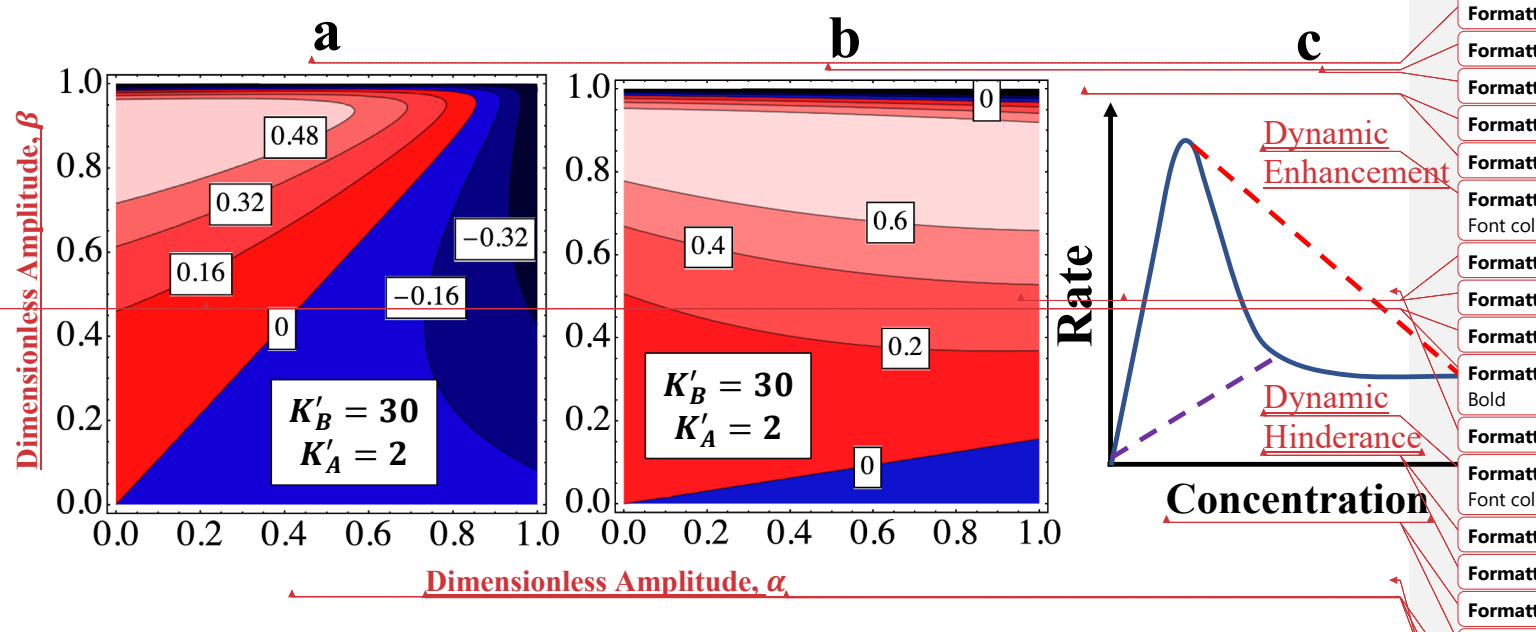


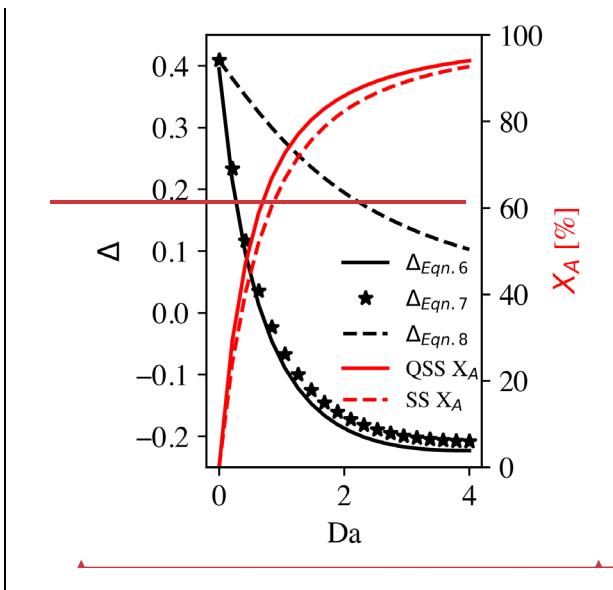
Figure 23: Fractional Fractional rate enhancement for simultaneous (a) and out—of—phase (b) modulation as functions of dimensionless amplitudes with $K'_1 = 2$ and $K'_2 = 30$ (c) QSS chords on a rate versus concentration for a second order denominator LH expression.

Formatted: Font: (Default) Times New Roman Formatted: Font: (Default) Times New Roman, 16 pt, Font color: Red Formatted: Font: (Default) Times New Roman, Bold Formatted: Font: (Default) Times New Roman Formatted: Font: Bold Formatted: Font: (Default) Times New Roman, 14 pt, Formatted: Centered Formatted: Font: (Default) Times New Roman, 16 pt, Font color: Purple Formatted: Font: 16 pt, Font color: Purple **Formatted** Formatted: Font: (Default) Times New Roman, Bold Formatted: Font: Bold Formatted: Font: (Default) Times New Roman Formatted: Font: Bold **Formatted** Formatted: Centered Formatted: Font: (Default) Times New Roman

Formatted: Right: 0.25"

Formatted: Font: (Default) Times New Roman
Formatted: Font: (Default) Times New Roman

Formatted: Justified



Formatted: Font: (Default) Times New Roman

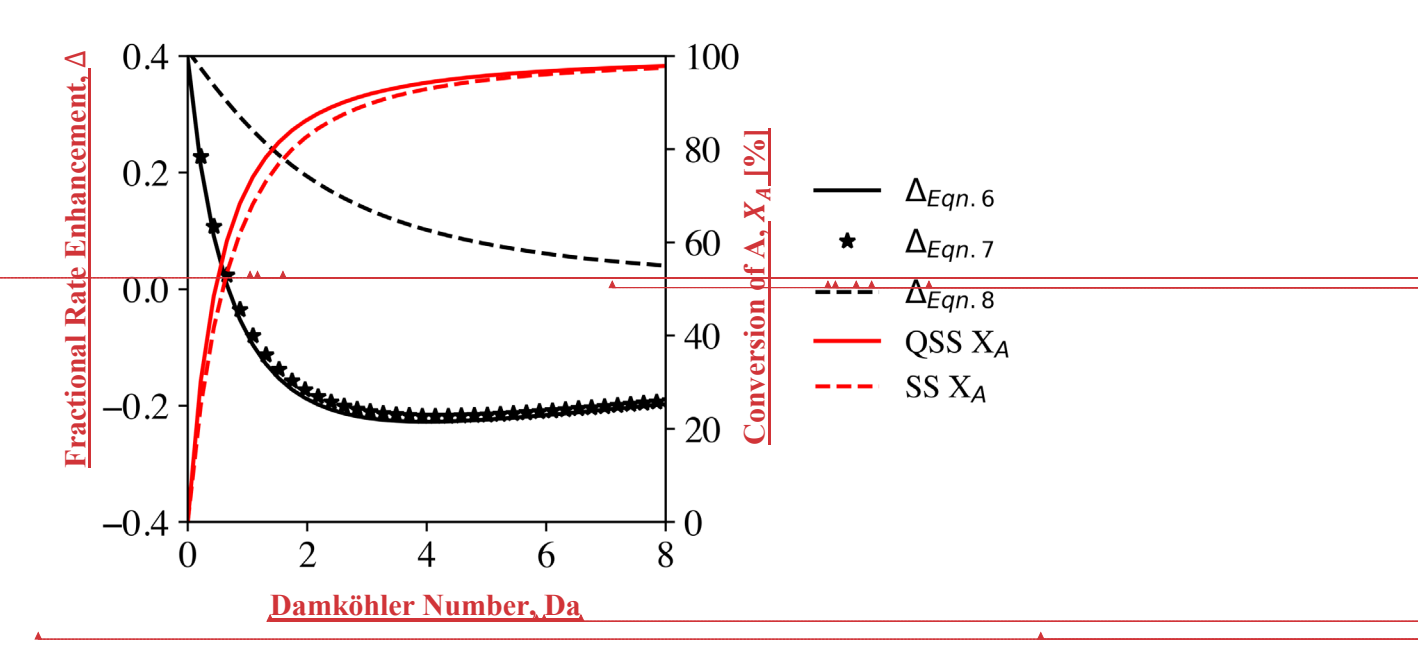


Figure 34: Local fFractional enhancement (Δ) calculated from Eqn. (6), Eqn. (7), and Eqn. (8) Eqn. (8) Eqn. (65 (__), Eqn. 67 (*) and Eqn. 78 (___) as functions of Da. Also shown is the calculated Percent conversion (X_i) [%] for of QSS (__) and SS (__) operation. For the case, as functions of Da (Δ). $x_{A,Avg,\Theta}^f = 1$, $x_{B,Avg,\Theta}^f = 2$, $x_{A,Avg,\Theta}^f = 3$, $x_{A,\Theta}^f = 3$, x_{A,Θ

Formatted: Font: (Default) Times New Roman

Formatted: Font: (Default) Times New Roman, Bold

Formatted: Font: Bold

Formatted: Font: (Default) Times New Roman, Bold

Formatted: Font: (Default) Times New Roman, 14 pt,

.

Formatted: Centered

Formatted: Font: Bold, Font color: Red

Formatted: Font: (Default) Times New Roman, Bold,

Font color: Red

Formatted: Font color: Red

Formatted: Font color: Red

Formatted: Font: Bold, Font color: Red

Formatted: Font: (Default) Times New Roman, 14 pt,

Bold, Font color: Red

Formatted: Centered

Formatted: Font: Bold

Formatted: Font: (Default) Times New Roman, Bold

Formatted: Font: Bold

Formatted: Font: (Default) Times New Roman, 14 pt,

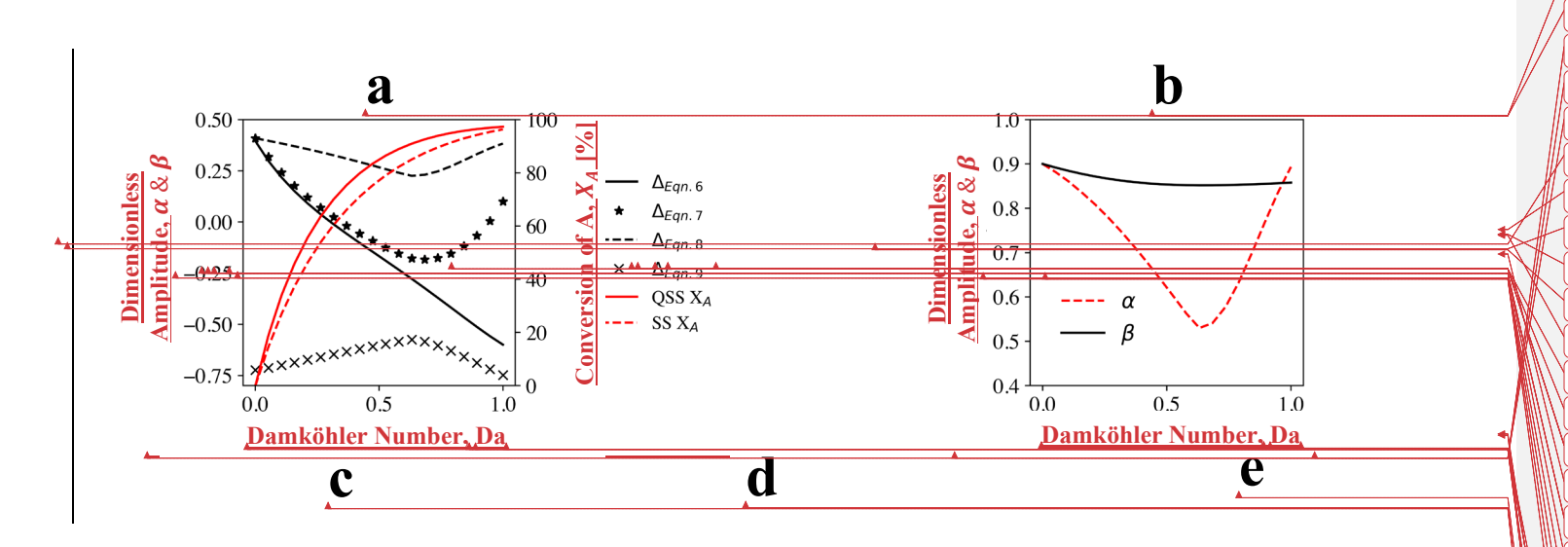
Bold

Formatted: Centered

Formatted: Font: (Default) Times New Roman

Formatted: Font: (Default) Times New Roman

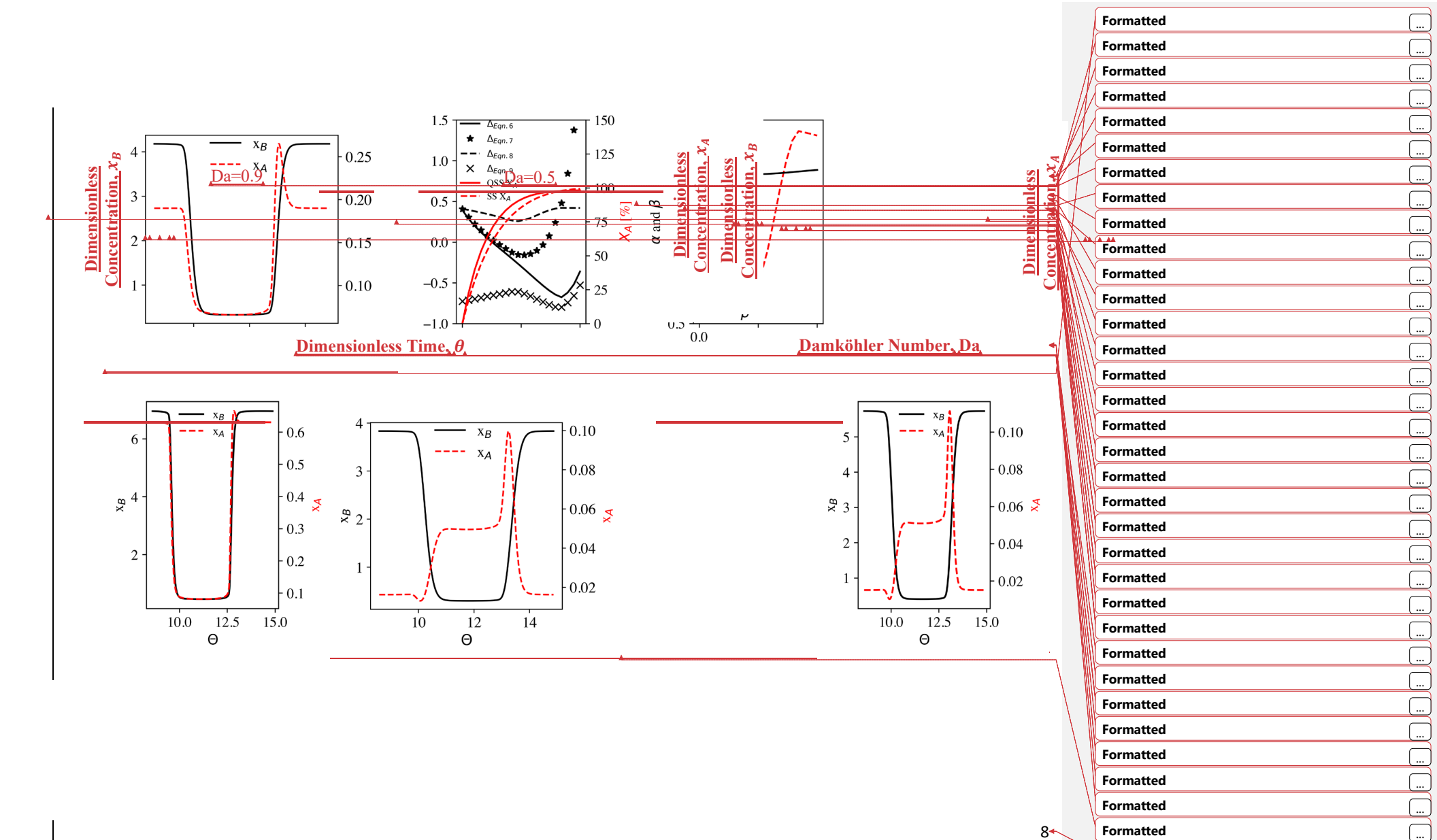
Formatted: Font: (Default) Times New Roman



Formatted	
Formatted	
Formatted	
Formatted	[
Formatted	[
Formatted	
Formatted	
Formatted	(
Formatted	
Formatted	(
Formatted	[
Formatted	
Formatted	(
Formatted	(
Formatted	(
Formatted	
Formatted	
Formatted	[
Formatted	[
Formatted	[
Formatted	
Formatted	
Formatted	[
Formatted	
Formatted	[
Formatted	

Formatted

C



Formatted

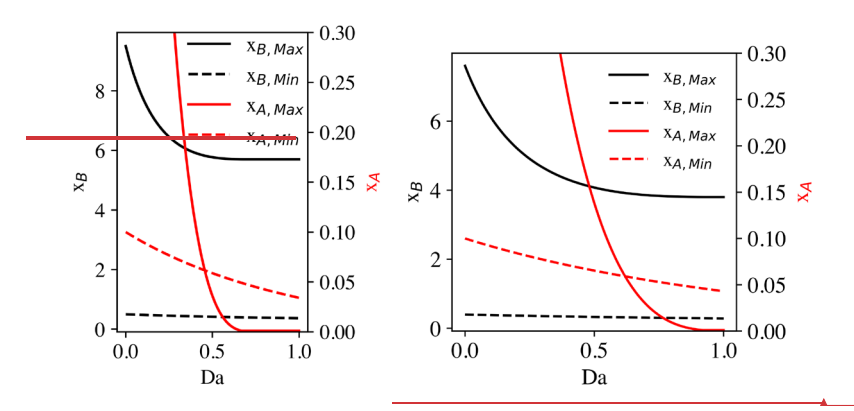
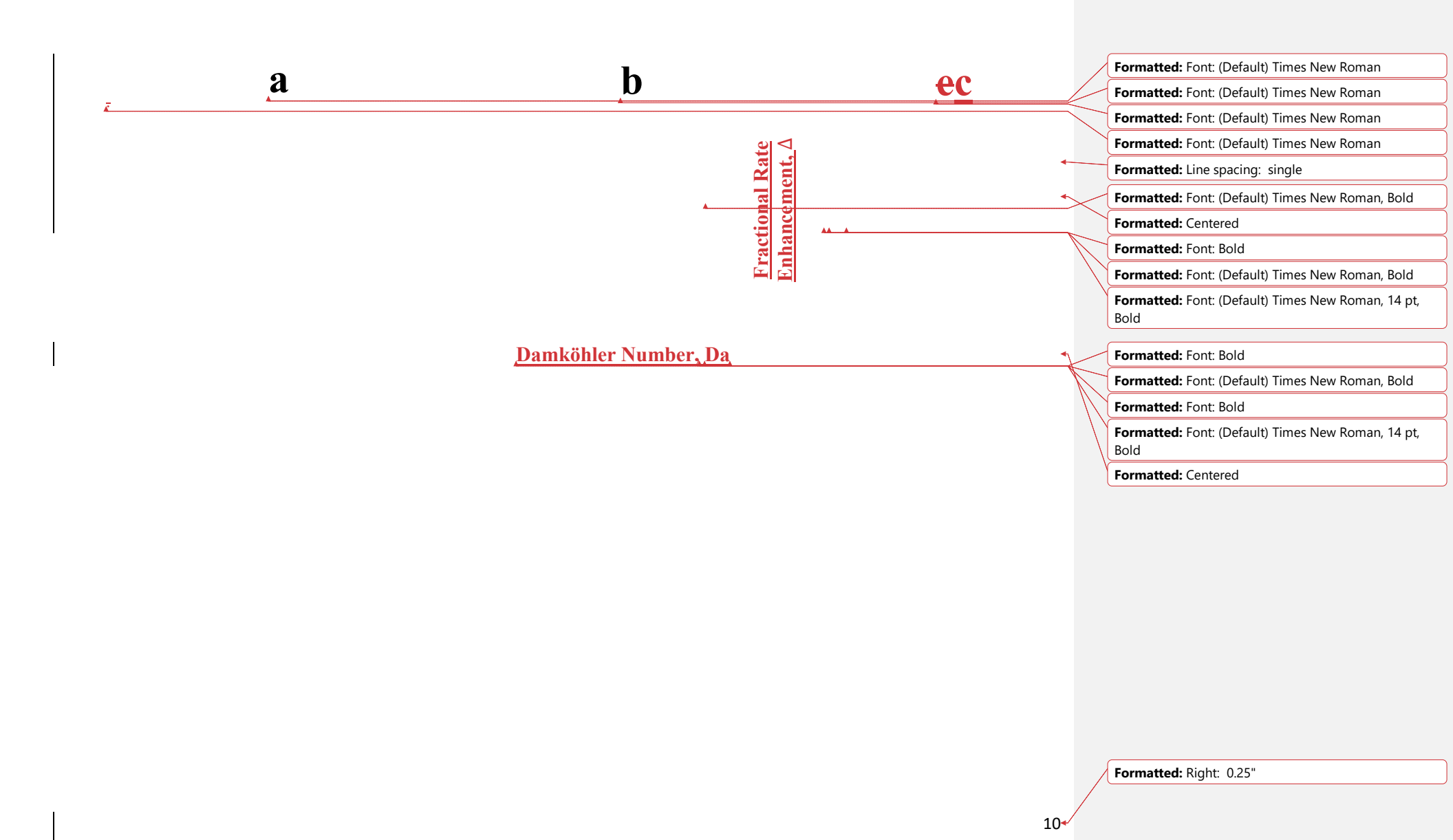
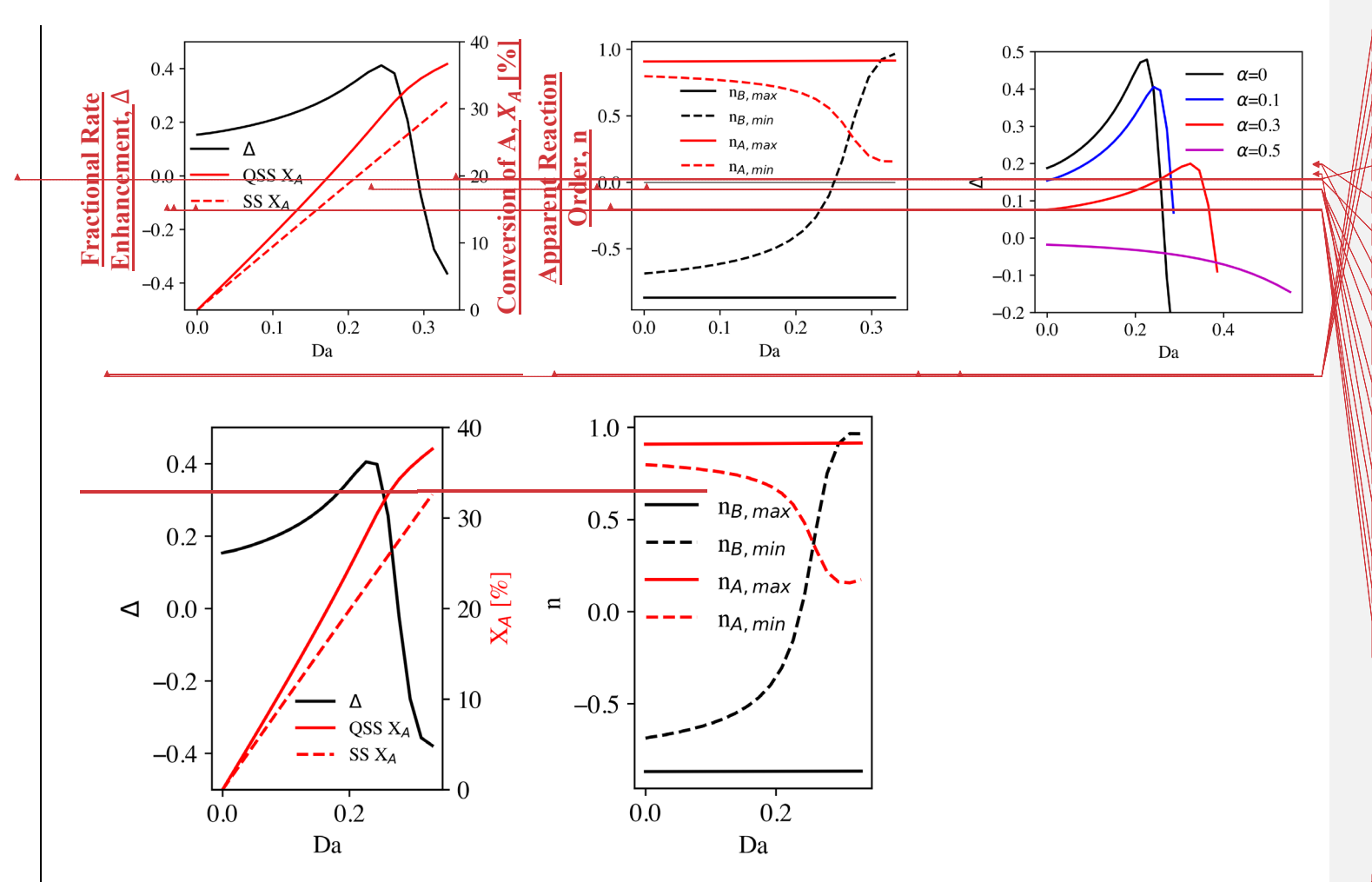


Figure 45: (a) Local fFractional enhancement (Δ) calculated from Eqn. (6)5 (...), Eqn. (7)6 (*), and Eqn. (8),7 (...) and Eqn. (9) as functions of Da. Percent conversion (X_{ij} [%] of QSS (...) and SS (...) operation as functions of Da (a). Where $x_{A,Avg,\oplus}^f = 1$, $x_{B,Avg,\oplus}^f = 45$, $\alpha_{\oplus}^f = \beta_{\oplus}^f = 0.9$, $s_A^f = s_B^f = 0.5$, n=0.7 and m=0.9 (a). (b) Dimensionless amplitudes, α (...) and β (...) versus Da (b). Dimensionless concentrations of A, x_A (...) and B, x_B (...) at $Da_a=0.52$ (c) and $Da_a=0.90.7$ (d). (e) Dimensionless reactant concentrations of species A (..., ...) and B (..., ...) at the wave maxima (..., ...) and minima (..., ...) as functions of Da solved through the SS design equations (e).

Formatted: Font: (Default) Times New Roman





Formatted: Font: (Default) Times New Roman

Formatted: Font: (Default) Times New Roman

Formatted: Font: (Default) Times New Roman

Formatted: Font: Bold

Formatted: Centered

Formatted: Font: (Default) Times New Roman, Bold

Formatted: Centered

Formatted: Font: Bold, Font color: Red

Formatted: Font: (Default) Times New Roman, Bold,

Font color: Red

Formatted: Font: Bold, Font color: Red

Formatted: Font: (Default) Times New Roman, 14 pt,

Bold, Font color: Red

Formatted: Centered

Formatted: Font: (Default) Times New Roman, 14 pt,

Bold

Formatted: Font: Bold

Formatted: Font: (Default) Times New Roman, Bold

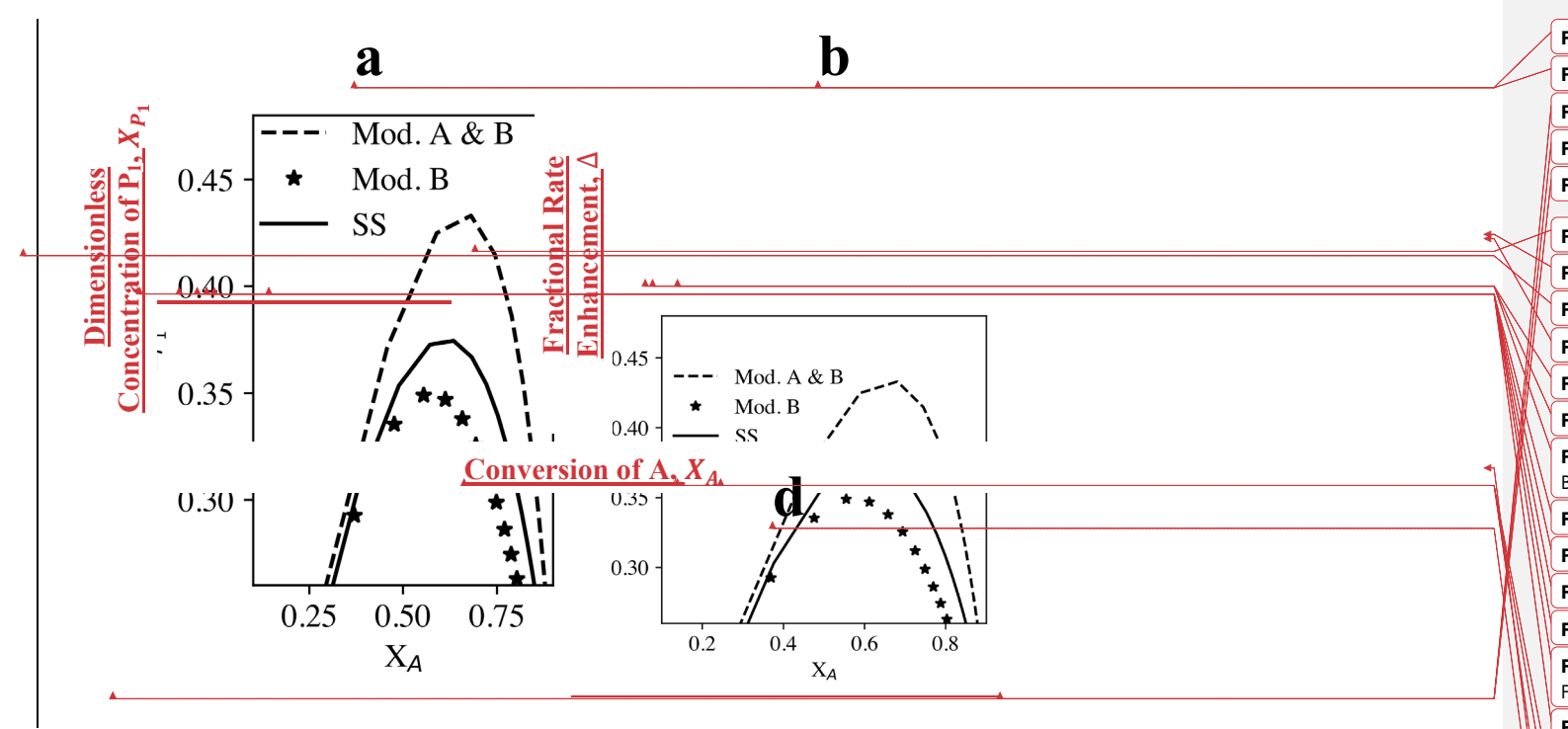
Formatted: Font: (Default) Times New Roman, 14 pt,

Bold

Figure 56:-(a) (a) Local fractional rate enhancement and conversions as functions of Da. (b) (b)-Apparent orders (c) as functions of Da for the steady state problem at the concentration wave maxima and minima. Plots are evaluated during simultaneous modulation where $x_{A,Avg}^f = 1$, $x_{B,Avg}^f = 1$, $x_{A}^f = 2$, $x_{B}^f = 30$, $x_{A}^f = 5$, $x_{B}^f = 0.5$, $x_{A}^f = 0.1$ and $x_{A}^f = 0.5$. (c) Fractional rate enhancement as a function of Da for different values of x_{A}^f in the range 0-0.5.

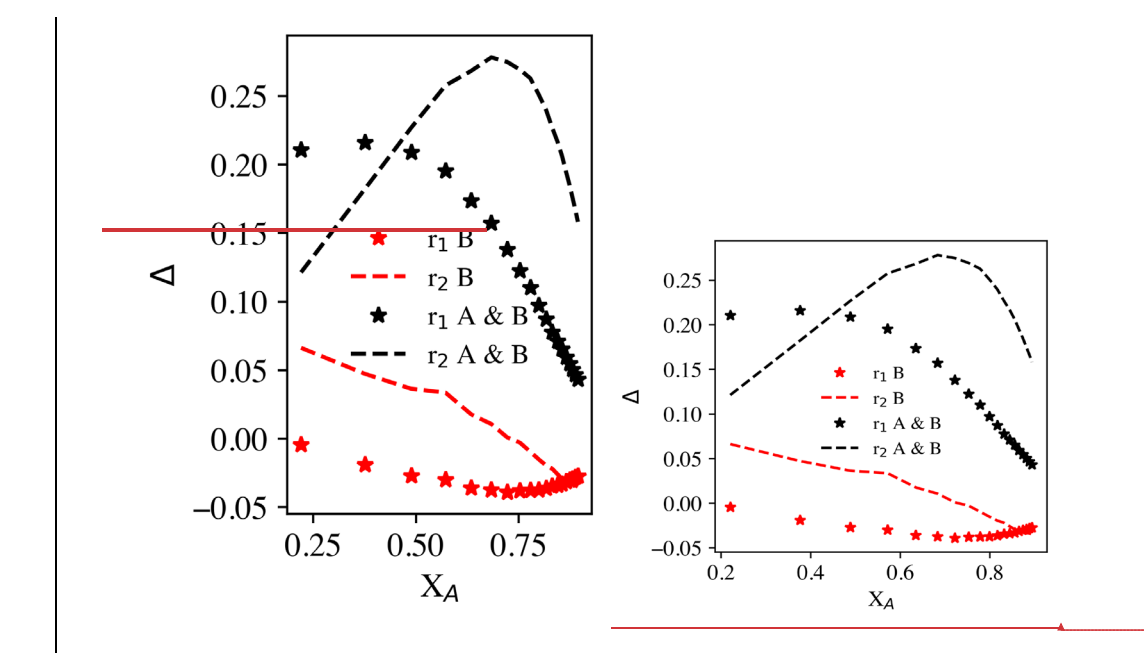
Commented [HMP4]: ??

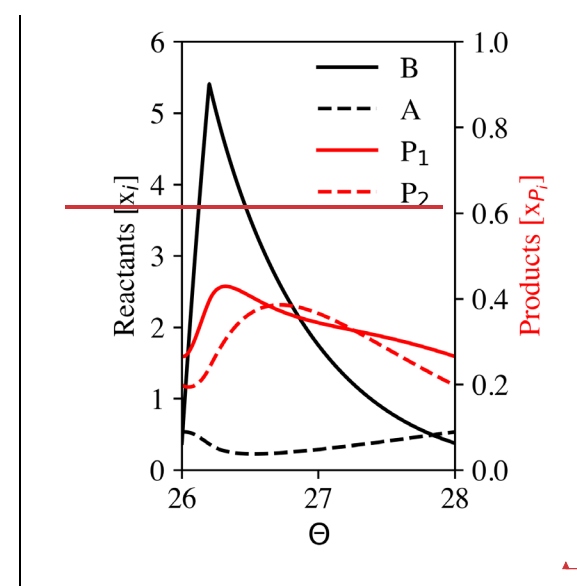
Formatted: Font: (Default) Times New Roman

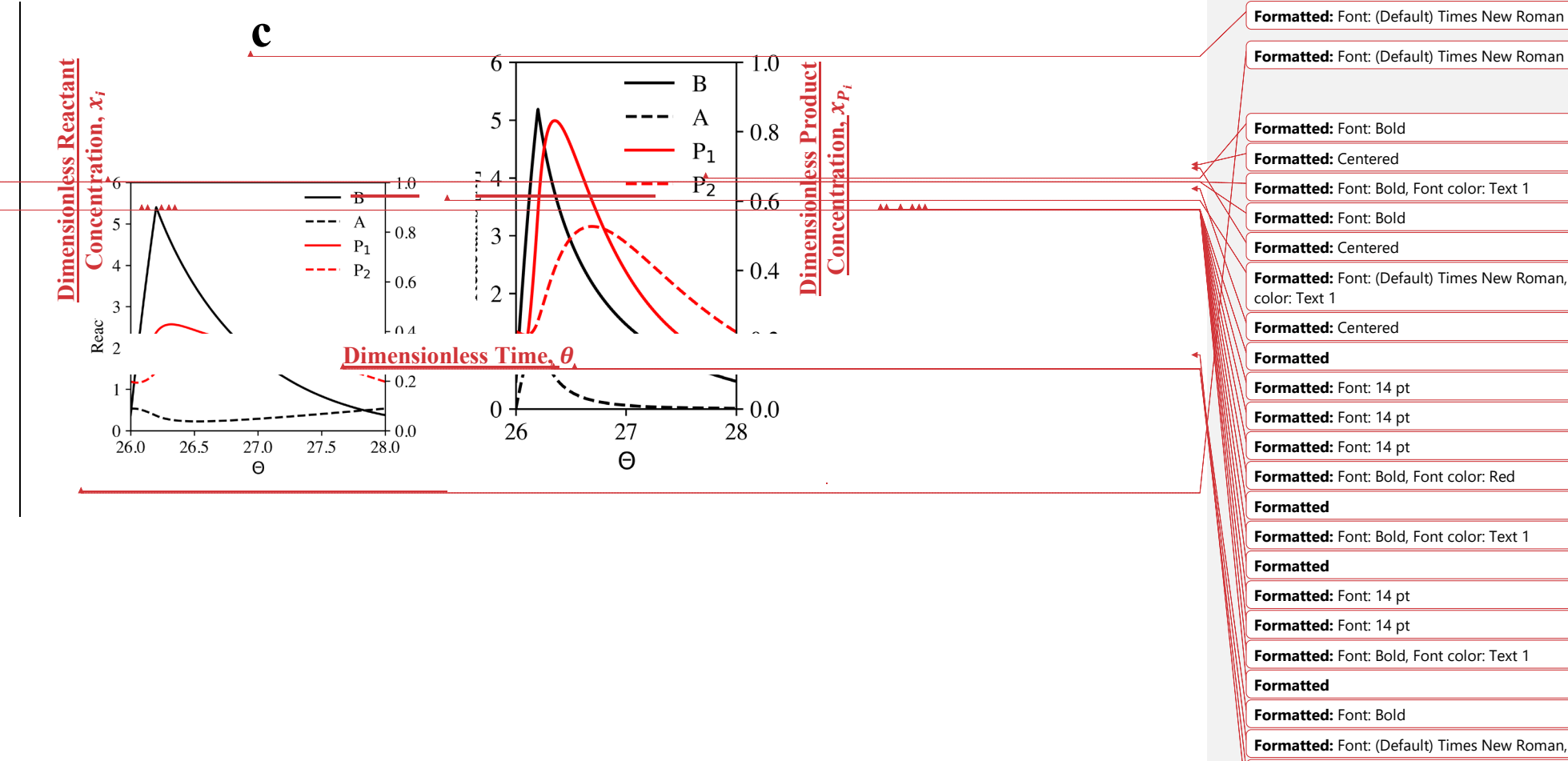


Formatted: Font: (Default) Times New Roman Formatted: Font: (Default) Times New Roman, Bold Formatted: Centered Formatted: Font: Bold Formatted: Centered Formatted: Font: Bold Formatted: Font: (Default) Times New Roman, Bold Formatted: Font: (Default) Times New Roman, 14 pt, Formatted: Font: Bold, Font color: Text 1 Formatted: Font: Bold Formatted: Font: Bold, Subscript Formatted: Font: Bold, Font color: Text 1 Formatted: Font: (Default) Times New Roman, Bold, Font color: Text 1 Formatted: Font: (Default) Times New Roman, 14 pt, Bold, Font color: Text 1 Formatted: Font: Bold, Font color: Text 1 Formatted: Font: (Default) Times New Roman, Bold, Font color: Text 1 **Formatted** Formatted: Centered

Formatted: Font: (Default) Times New Roman







Formatted: Font: (Default) Times New Roman	
Formattade Forte Bold	
Formatted: Font: Bold	
Formatted: Centered	
Formatted: Font: Bold, Font color: Text 1	
Formatted: Font: Bold	
Formatted: Centered	
Formatted: Font: (Default) Times New Roman, Font color: Text 1	
Formatted: Centered	
Formatted	[
Formatted: Font: 14 pt	
Formatted: Font: 14 pt	
Formatted: Font: 14 pt	
Formatted: Font: Bold, Font color: Red	
Formatted	<u></u>
Formatted: Font: Bold, Font color: Text 1	
Formatted	[
Formatted: Font: 14 pt	
Formatted: Font: 14 pt	
Formatted: Font: Bold, Font color: Text 1	
Formatted	[
Formatted: Font: Bold	
Formatted: Font: (Default) Times New Roman, Bold	
Formatted	(
Formatted: Centered	
Formatted: Right: 0.25"	

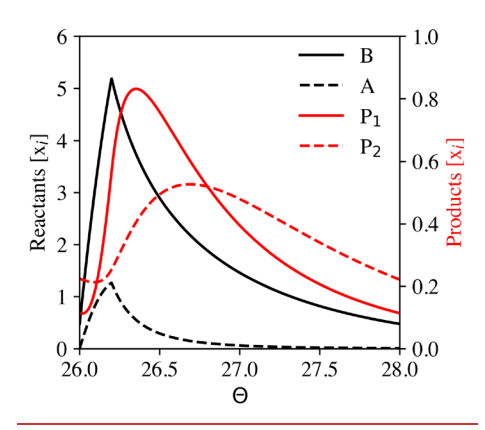
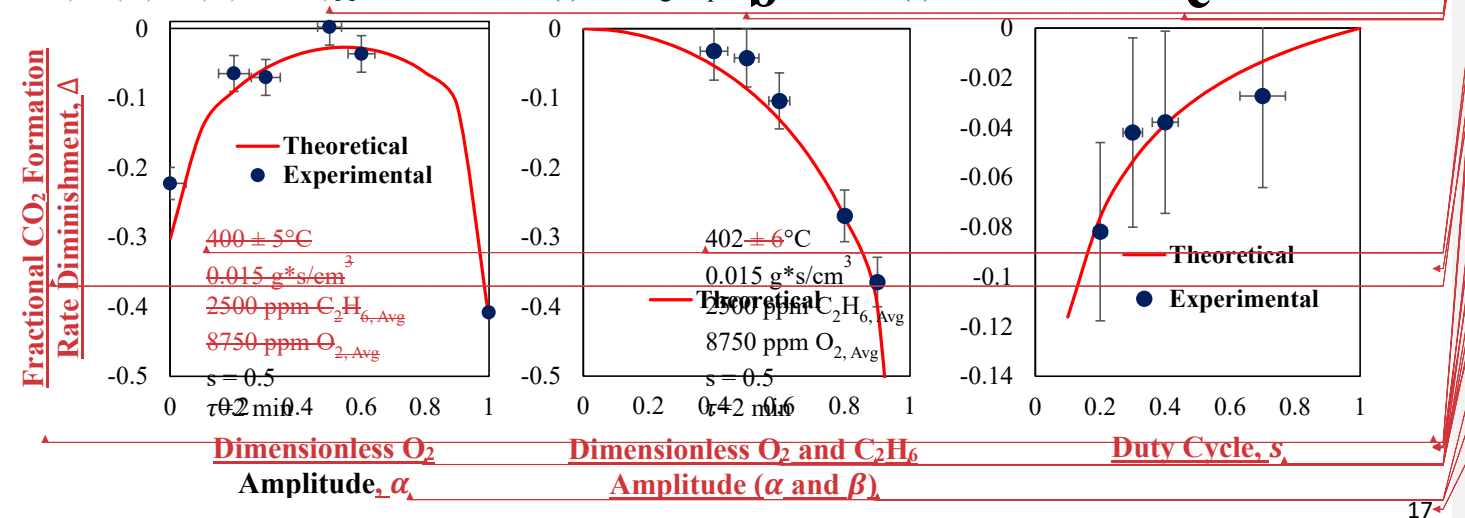


Figure $\frac{7}{5}$:6 (a) (a) Dimensionless P_1 concentration as a function of A converted for steady state (____), simultaneous (____, A & B) and single (\star , B only) reactant modulation reconstructed from Lee and Bailey [11]. (b) Fractional rate enhancement for r_1 (\star) for simultaneous (black) and single (red) species modulation. Dimensionless reactant concentration profiles during one period for A-(____), B-(___), P_1 (___) and P_2 (___) for simultaneous (c) and single species modulation (d).



Commented [AM5]: Ask Prof. about Fig. 7A as it is very similar to Bailey's work and perhaps we should mention that in this caption.

Formatted: Font: (Default) Times New Roman

Formatted: Font: 12 pt

Formatted: Font: 12 pt

Formatted: Font: (Default) Times New Roman, 14 pt,

Bold, Font color: Text 1

Formatted: Centered

Formatted: Font: (Default) Times New Roman, 14 pt,

Bold, Font color: Text 1

Formatted: Centered

Formatted: Subscript

Formatted: Centered

Formatted: Subscript

Formatted: Subscript

Formatted: Subscript

Formatted: Centered

Formatted: Font: (Default) Times New Roman, 14 pt,

Bold, Font color: Text 1

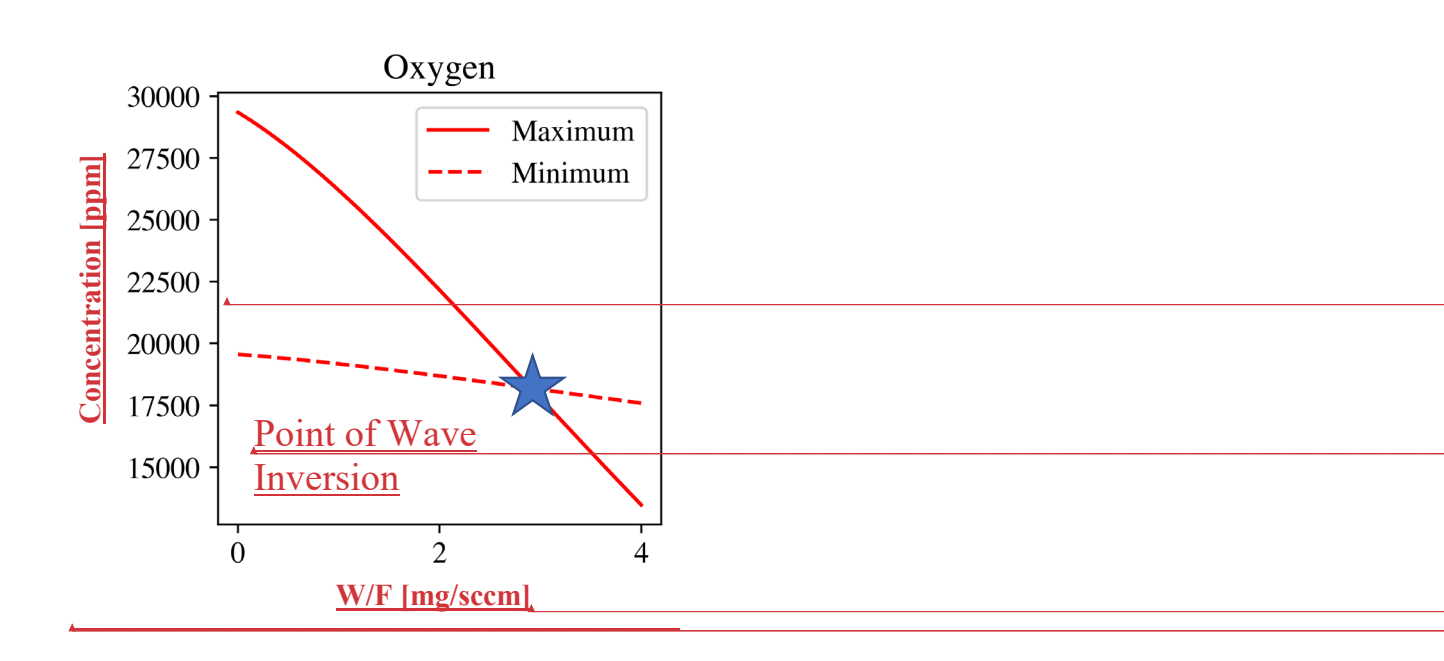
Formatted: Font: (Default) Times New Roman, 14 pt,

Bold, Font color: Text 1

Formatted: Right: 0.25"

Formatted: Font: 12 pt

Figure 786: Percent enhancement [%] of CO₂ formation rate for ethane oxidation for various dimensionless amplitudes determined experimentally (blue circles) and by eqn. eqns. 6 and (7) (red line). The simultaneous and out-of-phase experiments were carried out at 50% duty cycle (s=0.5) and period of 2 minutes (τ =2 min). (a) Simultaneous experiments were compared along the cross section, β = 1 – α , (b) Out-of-phase operation experiments were compared along the β = α , diagonal. (c) Duty cycle experiments were carried out with at α =0.5 and period of 3 minutes (τ =3 min). For all experiments the cyclic averages were 2500 and 8750 ppm of O₂ and C₂H₆ respectively and were carried out at 400°C with W/F=0.00157 g*ss/cm³ (200secm and 50 mg of catalyst).



Formatted: Font: (Default) Times New Roman

Formatted: Font: (Default) Times New Roman, 14 pt, Bold. Font color: Text 1

Formatted: Centered

Formatted: Font: (Default) Times New Roman, 18 pt

Formatted: Font: (Default) Times New Roman, 14 pt, Bold, Font color: Text 1

Formatted: Centered

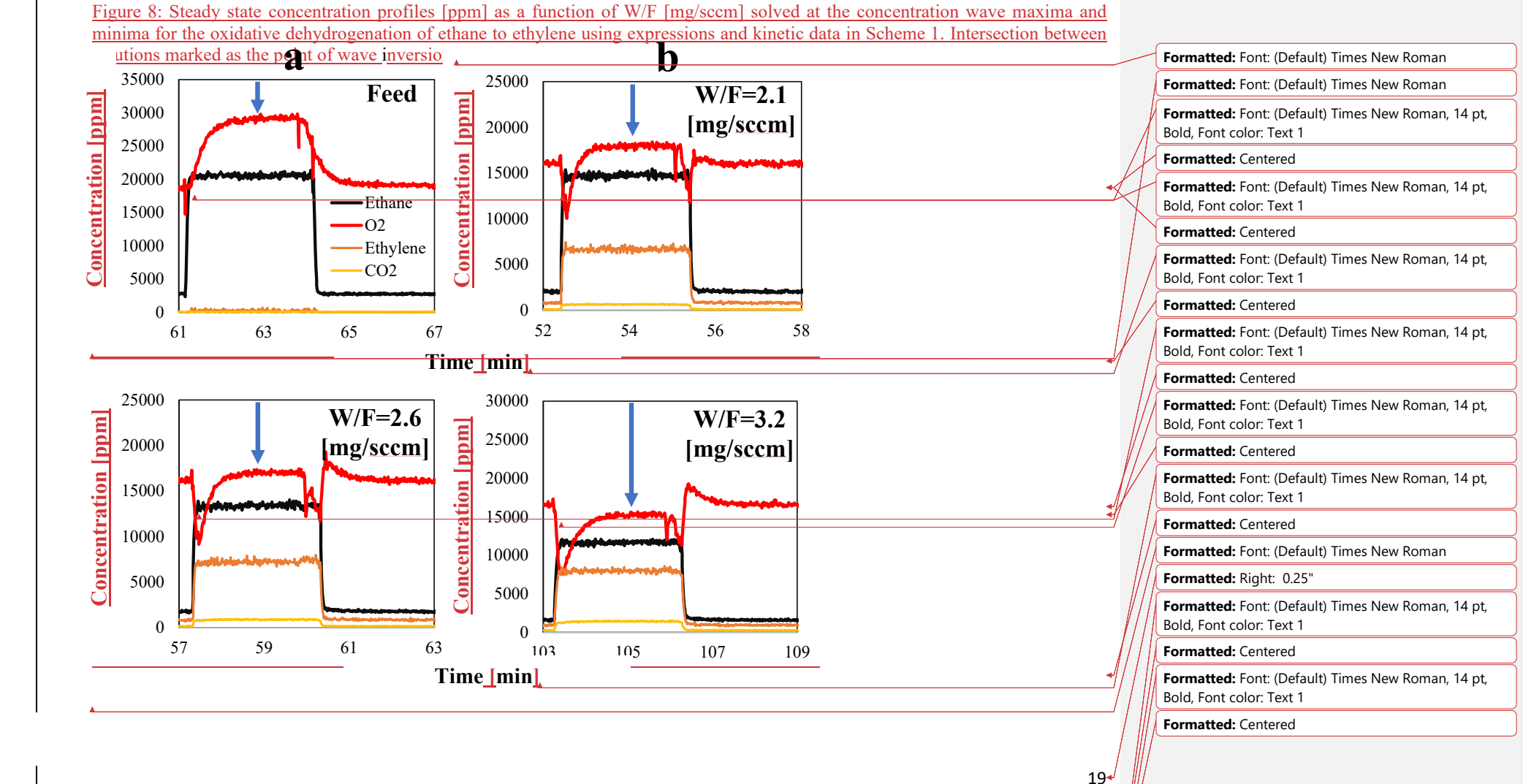


Figure 9: Seh Experimentally measured concentration profiles of O₂, C₂H₆, CO₂ and C₂H₄ at W/F = 0 (feed) (a), 2.1 (b), 2.6 (c), 3.2 (d) mg/sccm at 590°C period of 6 minutes and 50% duty cycle using 7wt% MoO₃Al₂O₃.

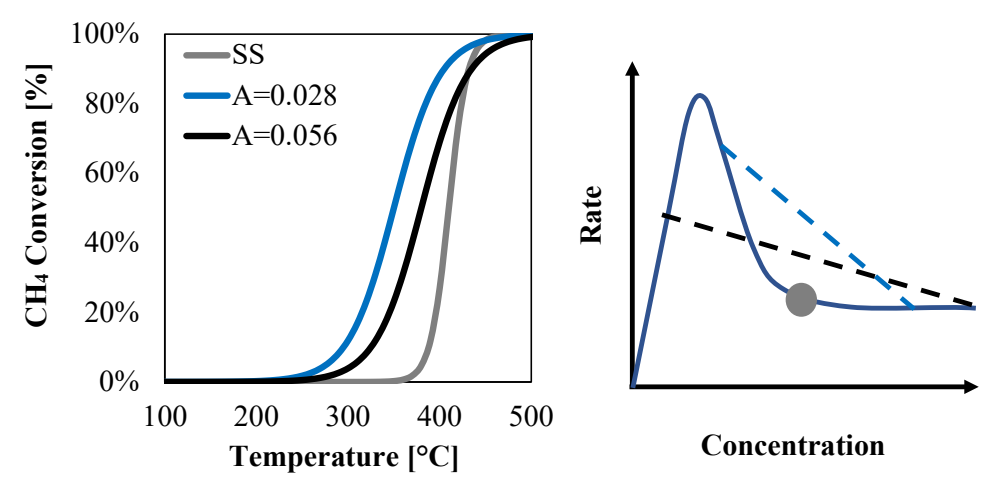


Figure 10: Methane conversion as a function of temeprature [°C] at different amplitudes during QSS operation of methane oxidation over supported Pt/Pd (PGM) catalysts (a). Rate of methane oxidation as a function of O₂ concentration (b). Figures are recreated from work by Karinshak *et. al.* [28].

Formatted: Font: (Default) Times New Roman	
Formatted	
Formatted	
Formatted	<u></u>
Formatted	
Formatted	
Formatted	
Formatted	<u></u>
Formatted	
Formatted	
Formatted	<u></u>
Formatted	<u></u>
Formatted	<u></u>
	<u> </u>
Formatted	
Formatted	[
Formatted	

Formatted